# Δ40p53 isoform up-regulates netrin-1/UNC5B expression and potentiates netrin-1 pro-oncogenic activity

Yan Sun, Ambroise Manceau, Lisa Frydman, Lucie Cappuccio, David Neves, Valeria Basso, Hong Wang, Joanna Fombonne, Carine Maisse, Patrick Mehlen, et al.

▶ **To cite this version:**

Yan Sun, Ambroise Manceau, Lisa Frydman, Lucie Cappuccio, David Neves, et al.. Δ40p53 isoform up-regulates netrin-1/UNC5B expression and potentiates netrin-1 pro-oncogenic activity. Proceedings of the National Academy of Sciences of the United States of America, 2021, 118 (36), pp.e2103319118. 10.1073/pnas.2103319118 . hal-03357293

**HAL Id: hal-03357293**
**https://hal.science/hal-03357293v1**

Submitted on 28 Sep 2021

**HAL** is a multi-disciplinary open access archive for the deposit and dissemination of scientific research documents, whether they are published or not. The documents may come from teaching and research institutions in France or abroad, or from public or private research centers.

L'archive ouverte pluridisciplinaire **HAL**, est destinée au dépôt et à la diffusion de documents scientifiques de niveau recherche, publiés ou non, émanant des établissements d'enseignement et de recherche français ou étrangers, des laboratoires publics ou privés.

# Δ40p53 isoform up-regulates netrin-1/UNC5B expression and potentiates netrin-1 pro-oncogenic activity

Yan Sun[a], Ambroise Manceau[a,1], Lisa Frydman[a,1], Lucie Cappuccio[b], David Neves[c], Valeria Basso[a], Hong Wang[a], Joanna Fombonne[a], Carine Maisse[b], Patrick Mehlen[a,2], and Andrea Paradisi[a,2]

[a]Apoptosis, Cancer and Development Laboratory - Equipe labellisée 'La Ligue', LabEx DEVweCAN, Centre de Recherche en Cancérologie de Lyon, INSERM U1052-CNRS UMR5286, Université de Lyon, Université Claude Bernard Lyon1, Centre Léon Bérard, 69008 Lyon, France.

[b]IVPC UMR754 INRAE, Université de Lyon, Université Claude Bernard Lyon1, EPHE, Lyon, France.

[c]Netris Pharma, 69008 Lyon.

[1]A.M. and L.F. contributed equally to this work.

[2]To whom correspondence may be addressed. Email: andrea.paradisi@lyon.unicancer.fr or patrick.mehlen@lyon.unicancer.fr.

**Corresponding authors addresses:** Andrea Paradisi (andrea.paradisi@lyon.unicancer.fr) and Patrick Mehlen (patrick.mehlen@lyon.unicancer.fr), Apoptosis, Cancer and Development Laboratory, Centre de Recherche en Cancérologie de Lyon, Centre Léon Bérard, 69008 Lyon, France. Phone: +33 (0)478782870.

**Classification**: BIOLOGICAL SCIENCES, Cell Biology

**Keywords:** apoptosis, netrin-1, p53 isoform

## Abstract

Netrin-1, a secreted protein recently characterized as a relevant cancer therapeutic target, is the anti-apoptotic ligand of the dependence receptors DCC and members of the UNC5H family. Netrin-1 is over-expressed in several aggressive cancers where it promotes cancer progression by inhibiting cell death induced by its receptors. Interference of its binding to its receptors has been shown, through the development of a monoclonal neutralizing anti-netrin-1 antibody (currently in phase II of clinical trial), to actively induce apoptosis and tumor growth inhibition. The transcription factor p53 was shown to positively regulates netrin-1 gene expression. We show here that netrin-1 could be a novel target gene of the N-terminal p53 isoform Δ40p53, independently of full-length p53 activity. Using stable cell lines, harboring wild-type or null-p53, in which Δ40p53 expression could be finely tuned, we prove that Δ40p53 binds to and activates the netrin-1 promoter. In addition, we show that forcing immortalized human skeletal myoblasts to produce the Δ40p53 isoform, instead of full-length p53, leads to the up-regulation of netrin-1 and its receptor UNC5B and promotes cell survival. Indeed, we demonstrate that netrin-1 interference, in presence of Δ40p53, triggers apoptosis in cancer and primary cells, leading to tumor growth inhibition in preclinical in vivo models. Finally, we show a positive correlation between netrin-1 and Δ40p53 gene expression in human melanoma and colorectal cancer biopsies. Hence, we propose that inhibition of netrin-1 binding to its receptors, should be a promising therapeutic strategy in human tumors expressing high levels of Δ40p53.

## Significance Statement

Netrin-1 is frequently over-expressed in aggressive cancers, acting as the anti-apoptotic ligand of the dependence receptors DCC and members of UNC5H family. Accordingly, netrin-1 inhibition induces apoptosis and tumor growth inhibition. We have shown that the transcription factor p53 regulates netrin-1 gene expression in cancer cells treated with conventional chemotherapeutic drugs. We demonstrate here that netrin-1 is a target gene of the N-terminal p53 isoform Δ40p53, acting independently of full-length p53 activity, thus promoting cell survival. Indeed, we show that netrin-1 interference, in presence of Δ40p53, triggers apoptosis in cancer and primary cells and tumor growth inhibition in preclinical in vivo models. Hence, we propose that netrin-1 inhibition should be a promising therapeutic strategy in tumors expressing high levels of Δ40p53.

## Introduction

Several studies have highlighted the crucial role of the secreted protein netrin-1 as an original cancer biomarker and therapeutic target (1-3). Initially discovered as an axon guidance cue during neuronal development, netrin-1 is also involved in cell survival and tumorigenesis (4). Indeed, netrin-1 receptors Deleted in Colorectal Carcinoma (DCC) and UNC5 homologue (UNC5H, *i.e.* UNC5A-D), belonging to the growing family of dependence receptors (5), induce “positive” signals upon ligand binding leading to differentiation and cell survival, and trigger apoptosis when unbound (6). Hence, cell survival depends on the presence of ligands of dependence receptors, the latter representing ideal tumor suppressors candidates. Indeed, the current hypothesis is that the expression of such a receptor represents a protective mechanism that limits tumor development. This could be achieved via the induction of apoptosis of tumor cells that would grow in or migrate to regions of limited ligand availability (7). Consequently, cell transformation towards a malignant or metastatic phenotype likely relies either on the loss of dependence receptors expression or on the constitutive inhibition of apoptosis induced by these receptors via ectopic ligand expression. Consistently, netrin-1 up-regulation has been described in several aggressive cancers (8-11), and is associated with tumor progression (8, 11, 12). The identification of netrin-1 as a tumor biomarker led to the development of an innovative personalized anti-cancer strategy. Indeed, interference of netrin-1 and its receptor binding induces apoptosis and favors tumor regression in several aggressive cancer models, expressing high netrin-1 levels (1, 8, 10-12). According to these findings, a humanized anti-netrin-1 antibody, called NP137, was developed (2) and

was assessed in a phase I clinical trial (https://clinicaltrials.gov/ct2/show/NCT02977195) and is now moving to a phase II clinical trial.

Despite the importance of netrin-1 in cell survival and cancer progression, little is known about the regulation of its expression. We formerly demonstrated that the transcription factor p53 was involved in the regulation of netrin-1 gene expression, following chemotherapy (1). p53 is a well-known tumor suppressor gene, through its ability to regulate the expression of different genes involved in a broad range of cellular responses, including apoptosis, cell cycle arrest, senescence and metabolism (13). p53 functions mainly depend on its ability to induce or repress transcription of target genes. However, transcription-independent activities of p53 have been described (14, 15). The transactivation activity of p53 requires two distinct transcriptional activation domains (TAD), encompassing residues 1-40 (TAD1) and 41-83 (TAD2) (16). Experiments in mice bearing inactivating point mutations in one or both TADs demonstrated a functional specialization of each TAD, that could regulate different target genes and effector pathways (17, 18). Interestingly, in the last few years, several alternative p53 transcripts were identified (19, 20). These protein isoforms are generated by different mechanisms, such as alternative splicing sites, promoters and translational initiation sites (21, 22). Some of these p53 isoforms lack TAD1 (Δ40p53) or both transactivation domains (Δ133p53) (20). The Δ40p53 isoform can be produced by alternative splicing, leading to the retention of intron 2 (23-25), or through the use of an alternative internal ribosomal entry sequence (IRES) at codon 40 (24). Conversely, the Δ133p53 isoform is generated from an internal promoter, located between intron 1 and exon 5, controlling the expression of a p53 mRNA sequence starting from intron 4 (19, 26).

Even though we previously showed that the full-length p53 (FLp53) directly binds to and activates the netrin-1 promoter (1), the molecular mechanisms underlying this regulation remain unclear. We reveal here that the regulation of netrin-1 and its main dependence receptor UNC5B requires the transactivation activity of p53 in tumor cells. Notably, netrin-1 transcriptional activation requires only p53 TAD2, unlike the majority of p53 target genes (17). Consequently, we show that Δ40p53, and not Δ133p53, can positively regulate netrin-1 and UNC5B gene expression, in a FLp53-independent manner. Moreover, we demonstrate that the expression of Δ40p53 and netrin-1 are correlated in human tumors. Finally, we speculate that treatment of tumor cells expressing Δ40p53 with neutralizing anti-netrin-1 antibody could be an innovative cancer therapeutic strategy.

## Results

### Netrin-1 regulation by p53 requires the transcriptional activity of the TAD2 domain

To unravel p53 regulation of netrin-1 expression, in particular the involvement or not of its transcriptional activity (14, 15), and possibly of its N-terminal transactivation domains (TADs) (17), we generated stable lung cancer H1299 cells bearing point mutations using sleeping beauty-based vectors. Indeed, site-specific L22Q and W23S mutations in TAD1 significantly inhibit the transcriptional activation of the p53 protein (27), whereas W53Q and F54S mutations inactivate TAD2 (Fig. 1A) (16). This methodology enabled us to activate wild-type or transcriptionally inactivated p53 mutants upon treatment with doxycycline of this p53-null cell line. Interestingly, basal protein levels of p53 mutants, in particular TAD1 mutants, were elevated compared to wild-type p53, likely due to the inhibition of Mdm2 ubiquitin ligase binding to p53 following the mutation of residues 22/23 (17, 27, 28). As previously shown (1), over-expression of wild-type p53 strongly induced netrin-1, as well as p21, a p53 target gene (Fig. 1B). However, while inactivation of p53 TAD1 ($p53^{22,23}$) did not affect netrin-1 protein expression, over-expression of the TAD2 mutant, alone ($p53^{53,54}$) or in combination with the TAD1 mutant ($p53^{22,23,53,54}$), blocked netrin-1 expression and that of its target gene p21 (Fig. 1B). This finding was further confirmed by quantitative RT-PCR (Fig. 1C), suggesting that netrin-1 up-regulation requires the transcriptional activity of p53, in particular the TAD2 domain.

### Δ40p53, but not Δ133p53, regulates netrin-1 and UNC5B gene expression

Some p53 alternative transcripts, generated by 5' splicing, IRES or alternative promoter, lack TAD1 (Δ40p53) or both TADs (Δ133p53) (Fig. 2A), similarly to the

transcriptional mutants generated above. We wondered whether different domains of the p53 N-terminal could regulate netrin-1 gene expression using known p53 isoforms. To this purpose, we generated stable lung cancer A549 lines, harboring wild-type p53, inducible for Δ40p53 or Δ133p53 isoforms and we analyzed gene expression by quantitative RT-PCR. Upon treatment with doxycycline, Δ40p53 over-expression strongly activated netrin-1 gene expression, whereas Δ133p53 induction had no effect (Fig. 2B, left panel), confirming results obtained with p53 transcriptional mutants. Interestingly, Δ40p53, but not Δ133p53, also up-regulated the main netrin-1 receptor, UNC5B (Fig. 2B, middle panel), and, despite the fact that Δ40p53 was reported to negatively modulate p21 (29, 30), we observed a positive regulation of p21 by Δ40p53 in our inducible cell lines (Fig. 2B, right panel). We confirmed the positive regulation of netrin-1 and p21 by Δ40p53 induction at the protein level by Western blot (Fig. 2C). It is of interest to note that in this model, Δ40p53 over-expression seemed to rather promote the p53 cell cycle arrest activity, as evidenced by p21 expression, compared to its pro-apoptotic function, since the BAX protein (Fig. 2C), another p53 target gene, remained unaffected.

To confirm that netrin-1 induction by Δ40p53 depends on its transcriptional activity, we conducted point mutations of residues W14 and F15 of Δ40p53 (Δ40p53$^{14,15}$), equivalent to positions 53 and 54 in FLp53 (see Fig. 2A). We then generated stable A549 cells inducible for wild-type Δ40p53 and Δ40p53$^{14,15}$ upon treatment with doxycycline, and we assessed protein and transcript levels by Western blot and quantitative RT-PCR analyses. Dysregulation of Δ40p53 transcriptional activity strongly inhibited netrin-1 and p21 protein expression upon doxycycline induction (Fig. 2D). Moreover, netrin-1, UNC5B

and p21 gene expression was very weak following Δ40p53[14,15] over-expression compared to Δ40p53 (*SI appendix*, Fig. S1).

Unlike H1299 cells, A549 cells harbor wild-type p53. We thus wondered whether the expression of Δ40p53 and Δ133p53 could affect endogenous FLp53 accumulation and activation upon Doxorubicin treatment and in turn affect netrin-1, UNC5B and p21 gene expression. We treated sleeping-beauty-modified A549 cells with doxycycline (to produce Δ40p53 or Δ133p53) and doxorubicin, and analyzed gene expression by quantitative RT-PCR. In Δ40p53-A549 cells, netrin-1, UNC5B and p21 gene expression was strongly up-regulated upon treatment with doxycycline and doxorubicin separately (Fig. 2E), confirming that Δ40p53 positively regulates these genes, and that endogenous FLp53, induced by doxorubicin, triggers netrin-1 and UNC5B gene expression (1). Interestingly, netrin-1 and UNC5B up-regulation increased further upon induction of Δ40p53, while in Δ133p53-A549 cells doxycycline treatment strongly inhibited netrin-1 and UNC5B induction by doxorubicin (Fig. 2E), confirming a dominant-negative role for Δ133p53 against FLp53 (19, 31). Intriguingly, p21 gene expression following doxorubicin treatment was suppressed by doxycycline in both Δ40p53- and Δ133p53-A549 cells (Fig. 2E), suggesting that, at least for p21, Δ40p53 may also act as a dominant-negative effector of FLp53.

**FLp53 is not necessary for netrin-1 regulation by Δ40p53**

Even though increasing evidence suggests that Δ40p53 may regulate gene expression independently of FLp53 (32-34), this isoform is also known to function as a FLp53 regulator, since Δ40p53 can oligomerize with FLp53, regulating its activities and

functions (24). To assess the involvement of FLp53 in Δ40p53-dependent regulation of netrin-1, we generated stable p53-null H1299 cells, inducible for Δ40p53, FLp53 or both proteins. Gene expression analysis upon doxycycline treatment revealed a robust induction of netrin-1 gene expression following over-expression of both p53 proteins (Fig. 3A). Moreover, co-expression of FLp53 and Δ40p53 did not significantly change netrin-1 expression, compared to separate inductions. We confirmed these results at the protein level by Western blot analysis (Fig. 3B).

To ascertain that Δ40p53 regulates netrin-1 *per se*, regardless of FLp53 expression, we silenced endogenous FLp53 expression in A549 cells inducible for Δ40p53, using a specific siRNA targeting exon 2 of the p53 gene -i.e., thus avoiding degradation of Δ40p53 mRNA (Fig. 3C)-. Cells were treated with doxorubicin, in addition to doxycycline to induce Δ40p53 expression, and FLp53 silencing was then verified by western blot and quantitative RT-PCR (Fig. 3C and *SI appendix*, Fig. S2A). Western blot and quantitative RT-PCR analysis showed a strong accumulation of netrin-1, UNC5B and p21 upon induction of Δ40p53 or doxorubicin treatment in cells transfected with control siRNA (Fig. 3 C and D, and *SI appendix*, Fig. S2A). Moreover, although FLp53 silencing completely abolished the increase in target gene expression observed in doxorubicin-treated cells, Δ40p53 was able to trigger netrin-1, UNC5B and p21 gene expression in these cells (Fig. 3 C and D, and *SI appendix*, Fig. S2A).

Finally, to validate the independence of Δ40p53 activity on netrin-1 with respect to FLp53 without relying on siRNA transfections, we stably repressed endogenous FLp53 in A549 cells inducible for Δ40p53, using CRISPR-dCas9-KRAB, a modified CRISPR/Cas9-based system (35). We designed small guide RNAs (sgRNAs), targeting the first canonical

p53 promoter, able to direct the binding of a nuclease defective Cas9 (dCas9) enzyme fused to KRAB (Krüppel-associated box) domain of Kox1 (35, 36). The KRAB domain leads to transcription repression of p53 isoforms whose expression is regulated by this promoter -*i.e.*, full-length and ∆40p53 isoforms (α, β and γ)- by mediating local epigenetic reprogramming of histone modifications (37, 38). FLp53 down-regulation was verified by Western blot analysis (Fig. 3E) in stably transfected A549 cells treated with doxorubicin. sgp53A completely inhibited basal and drug-induced FLp53 expression, while sgp53B showed a robust repression of FLp53 expression. Accordingly, netrin-1 up-regulation following doxorubicin treatment was completely inhibited in FLp53-repressed cells at protein and transcriptional levels (Fig. 3E and *SI appendix*, Fig. S2B), as well as its receptor UNC5B (*SI appendix*, Fig. S2C). However, ∆40p53 induction by doxycycline, not affected by dCas9-KRAB expression since it was regulated by a tetracycline-dependent CMV promoter, was still sufficient to trigger netrin-1 and UNC5B gene expression, even in the absence of FLp53 (Fig. 3E). Collectively, these results demonstrate that netrin-1 induction by ∆40p53 is independent of FLp53.

**∆40p53 directly binds and activates the netrin-1 promoter**

We then assessed whether ∆40p53 regulated netrin-1 via its promoter. Indeed, we previously cloned two different netrin-1 promoters (9, 39), and confirmed the presence of a p53 binding site in the internal netrin-1 promoter (1). Induction of FLp53 or ∆40p53 using doxycycline triggered transcription of firefly luciferase reporter gene placed under the control of the internal netrin-1 promoter or p21 promoter (Fig. 4A). However, site-direct

mutagenesis of p53 binding site in the netrin-1 promoter completely abolished promoter transactivation upon induction of both FLp53 and Δ40p53 (Fig. 4A).

As Δ40p53, similarly to FLp53, can activate the netrin-1 promoter using the same p53 binding site, we wondered whether Δ40p53 interacted with the netrin-1 promoter in the same region. To ascertain this, we performed a chromatin-immunoprecipitation assay, using stable H1299 cells inducible for Δ40p53. PCR results show that, upon immunoprecipitation of over-expressed Δ40p53, using anti-HA-tagged antibody, we amplified a DNA fragment surrounding the p53 binding site in the netrin-1 promoter (Fig. 4B). Moreover, we confirmed that Δ40p53 was also able to interact with the p21 promoter (Fig. 4B). Altogether, these results demonstrate that Δ40p53 can directly bind the netrin-1 promoter at the same binding site as FLp53, favoring its transcriptional activation.

**Endogenous Δ40p53 regulates netrin-1 expression**

Having shown that over-expression of Δ40p53 induces the expression of netrin-1 and its receptor UNC5B, we next studied the role of endogenously-produced Δ40p53 on netrin-1 regulation. To achieve this, we used immortalized human skeletal myoblasts LHCN-M2, harboring wild-type p53. We designed two different sgRNAs, targeting "canonical" ATG in p53 exon 2 (sgFLp53) or the ATG codon 40 in p53 exon 4 (sgTOTp53), in order to inactivate FLp53 (*i.e.*, p53α, β and γ) or FL/Δ40p53 (including Δ40p53α, β and γ) isoforms, respectively (Fig. 5A). Moreover, both sgRNAs should not affect the expression of Δ133p53 and Δ160p53 isoforms. Then, using the CRISPR-Cas9 technique, we generated stable LHCN-M2 cell lines. Western blot analysis revealed a complete knock-out of p53 isoforms in stable cells generated with sgTOTp53, whereas in cells set-

up with sgFLp53 only FLp53 was deleted (Fig. 5B). Moreover, in these cells a band corresponding to Δ40p53α appeared, demonstrating that this CRISPR-Cas9 strategy allowed us to force LHCN-M2 cells to produce endogenous Δ40p53 instead of FLp53. Interestingly, netrin-1 and UNC5B proteins were strongly expressed in LHCN-M2-sgFLp53 cells, harboring Δ40p53 instead of FLp53, compared to control or sgTOTp53 cells (Fig. 5B). Moreover, quantitative RT-PCR analysis confirmed an increase in netrin-1 expression in LHCN-M2 cells expressing endogenous Δ40p53 (Fig. 5C). Intriguingly, gene expression of p21 and GADD45 (p53 target genes involved in cell cycle arrest) strongly decreased in both FLp53 knock-out cells, compared to parental or control LHCN-M2 cells, while only complete p53 knock-out drove a decrease in BAX (involved in apoptotic function of p53) gene expression (Fig. 5C and *SI appendix*, Fig. S3).

**Δ40p53 expression intensifies netrin-1 dependence and sensitizes cells to netrin-1 silencing-induced apoptosis**

Since the over-expression or forced expression of Δ40p53 triggered an increase in the expression of netrin-1 and its receptor UNC5B, we hypothesized that in these cells survival dependency on netrin-1 expression may be amplified. To confirm this, we transfected stable LHCN-M2 cells with siRNA specific for netrin-1 (1). Netrin-1 silencing induced an increase in DNA fragmentation exclusively in sgFLp53 cells expressing endogenous Δ40p53 and consequently netrin-1 and UNC5B (Fig. 6A). Moreover, in these cells netrin-1 silencing induced a robust caspase-3 activation, compared to parental or control LHCN-M2 cells (Fig. 6B). Furthermore, complete p53 knock-out desensitized sgTOTp53 cells to netrin-1 silencing (Fig. 6 A and B). DNA fragmentation and caspase-3

activation observed in LHCN-M2 cells suggest that cell death triggered by netrin-1 silencing is apoptosis. Along the same line, transfection of siRNA targeting netrin-1 induced a consistent increase of the percentage of Annexin V positive cells only in sgFLp53 cells expressing endogenous Δ40p53α (Fig. 6C and *SI appendix*, Fig. S4). In line with these results, silencing netrin-1 increased DNA fragmentation upon induction of Δ40p53 in stable A549 cells (Fig. 6D), confirming the amplification of netrin-1 dependency in cells expressing high levels of Δ40p53. Interestingly, netrin-1 silencing had no effect on the induction of apoptosis in cells not treated with doxycycline (Fig. 6D).

**Netrin-1 interference inhibits tumor growth in tumors cells expressing Δ40p53 in vivo**

Because we observed that over-expression of Δ40p53, by inducing both netrin-1 and UNC5B, renders cancer cells more prone to die upon netrin-1 silencing, we next look whether this can be associated with tumor growth inhibition *in vivo*, using a more therapeutically-relevant approach. For this purpose, we evaluated the effect of NP137, a neutralizing anti-netrin-1 antibody able to induce cancer cell death and tumor regression in several preclinical models (2), upon Δ40p53 induction using the chicken chorioallantoic membrane (CAM) xenograft model. This technique is well accepted to study primary tumor growth on the highly vascularized CAM of chicken embryo (40, 41). Stable A549 cells inducible for Δ40p53 were engrafted into the CAM of E10 chicken embryos and primary tumors at the inoculation site were resected seven days after (Fig. 7A). In presence of doxycycline, Δ40p53α was induced (*SI appendix*, Fig. S5A) and anti-netrin-1 antibody (NP137) strongly reduced both the size and the weight of the tumors, compared to isotypic

antibody (Iso-mAb)-treated engrafted cells (Fig. 7 B and C). Moreover, treatment with NP137 antibody did not affect CAM tumor growth in PBS-treated cells, indicating that the antitumoral effect of netrin-1 interfering is dependent on Δ40p53 expression. Interestingly, production of Δ40p53 upon doxycycline treatment slightly sustained tumor growth, even though this increase was not significant, suggesting a pro-tumoral effect of Δ40p53/netrin-1 axis, that could be reverted by netrin-1 interference.

The antitumoral effect of anti-netrin-1 antibody was also confirmed in a more conventional preclinical model of *nude* mice, engrafted with stable A549 cells inducible for Δ40p53α. As observed for the CAM model, while we noticed a substantial tumor growth in mice treated with PBS or isotypic control, anti-netrin-1 antibody considerably inhibited tumor progression in mice watered with doxycycline (Fig. 7D and *SI appendix*, Fig. S5B). This effect was associated with apoptosis induction, as indicated by the increase of cleaved caspase-3 positive cells in engrafted tumors treated with both doxycycline and NP137 antibody (Fig. 7E and *SI appendix*, Fig. S5C).

Finally, we tested how endogenous Δ40p53 protein could affect sensitivity to netrin-1 inhibition. For this purpose, we used colorectal cancer HCT116 cells wild-type ($HCT116^{p53+/+}$) or deleted for FLp53 ($HCT116^{p53-/-}$) (42). Similar to the sgFLp53 LHCN-M2 cells we described above (see Fig. 5A), $HCT116^{p53-/-}$ cells were generated by deletion of exon 2 on p53 gene, resulting in FLp53 knock-out. So, in this setting the $HCT116^{p53+/+}$ parental cell line is expressing low level of wild-type FLp53 but no Δ40p53 protein, whereas $HCT116^{p53-/-}$ cells express no FLp53 but Δ40p53 protein (*SI appendix*, Fig. S6A). Of interest, $HCT116^{p53-/-}$ cells showed a significant increase of netrin-1 and UNC5B transcripts (*SI appendix*, Fig. S6B). Accordingly, transfection of siRNA targeting netrin-1

had no effect on cell viability in wild-type cells -*i.e.* supporting the view that low endogenous FLp53 does not regulate netrin-1/UNC5B activity- while it triggers DNA fragmentation exclusively in HCT116$^{p53-/-}$ cells (*SI appendix*, Fig. S6C). Moreover, NP137 antibody nicely decreased the size and the weight of tumors obtained from HCT116$^{p53-/-}$ cells on chicken CAMs (Fig. 7F and *SI appendix*, Fig. S6D).

**Netrin-1 and Δ40p53 gene expression is correlated in human tumor biopsies.**

We thus wondered whether Δ40p53 could positively regulate netrin-1 in a panel of human tumors. Indeed, conversely to FLp53, the activity of which is mainly regulated at a post-translational level in human cancers, Δ40p53 could be transcriptionally regulated and contribute to the neoplastic phenotype (29, 43-45). Moreover, netrin-1 is often dysregulated in cancers. For this purpose, we analyzed mRNA levels of netrin-1 and Δ40p53 gene expression in melanoma and colorectal cancer biopsies by quantitative RT-PCR. As shown in Fig. 8A, in both cohorts analyzed, we found a positive and significant correlation between netrin-1 and Δ40p53. Moreover, netrin-1 appeared more expressed in human tumor materials presenting high levels of Δ40p53 (Fig. 8B). These results support the view that in human tumors, netrin-1 could be positively regulated by Δ40p53.

## Discussion

Netrin-1 is a protein frequently up-regulated in aggressive human cancers (8-11). The pro-tumoral function of netrin-1 mainly results from its ability to bind dependence receptors DCC and UNC5H, inhibiting their pro-apoptotic activity (5, 46-49). Within this context, several studies have focused on inhibiting the binding of netrin-1 to its receptors to induce cancer cell death and tumor regression (2, 8, 10-12, 50). These attempts led to the development of a netrin-1 neutralizing antibody, currently in Phase Ib/II clinical trial (2). However, netrin-1 inhibition may only be applied to the fraction of tumors expressing high levels of netrin-1. Therefore, the knowledge of which cancer cells rely on this strategy to survive and what mechanisms underlie netrin-1 up-regulation in tumor cells could be important in developing personalized therapeutic treatments. Having shown that the transcription factor p53 positively regulates netrin-1 (1), we investigated the underlying mechanisms, as such knowledge could increase the fraction of cancer patients who may be eligible for a netrin-1 interference-based treatment during early clinical evaluation.

Here we demonstrate that ∆40p53, a N-terminal truncated isoform of p53, transcriptionally regulates the gene expression of netrin-1 and its receptor UNC5B, and unexpectedly, it does so independently of the presence of FLp53. Indeed, early studies reported ∆40p53 as a dominant-negative regulator of FLp53 (20), since its over-expression down-regulates FLp53-induced target genes, counteracting FLp53-dependent growth suppression (23, 24). However, ∆40p53 was more recently described as a positive regulator of FLp53 functions (30), since Δ40p53 over-expression induces apoptosis in melanoma cells in cells expressing wild-type FLp53 exclusively (29). These paradoxical results have been attributed to dose-dependent effects of hetero-oligomerization of p53

isoforms, dependent on the relative expression levels (51). For instance, it has been demonstrated that low Δ40p53 expression enhances FLp53 transactivation activity, whereas increasing levels suppress anti-proliferative effects of FLp53 (30). As a consequence, because netrin-1 was previously described as a FLp53 target gene (1), its regulation by Δ40p53 expression could have been due to p53 stabilization and activation by hetero-oligomers Δ40p53/FLp53. However, our results, showing netrin-1 up-regulation by Δ40p53 in H1299 p53-null cells or upon FLp53 knock-out in A549 p53-wild-type cells, suggest the formation of a Δ40p53-only homo-tetramer, binding to and activating netrin-1 promoter. On the other hand, binding of Δ40p53 to p53 responsive elements located in MDM2, GADD45 and BAX genes, leading to FLp53-independent transactivation, has been already reported (32). Interestingly, our data also show that the CRISPR-Cas9 technique, using specific sgRNAs, enabled us to generate stable primary cells expressing Δ40p53 instead of FLp53. In this way, we were also able to confirm the up-regulation of netrin-1 and UNC5B by endogenously-expressed Δ40p53. This information, together with gene expression analysis on inducible stable cell lines, suggests that Δ40p53 can establish homo-tetramers, transactivating the netrin-1 promoter, in the context of both high and low Δ40p53 expression levels, at least in the absence of FLp53.

p53 isoforms are differentially expressed in several human cancers (21, 52), such as triple-negative breast and mucinous ovarian cancers and melanoma (43-45). However, the high expression of Δ40p53 and correlated cancer aggressiveness has been associated with the dominant-negative function of this isoform on FLp53 activity. Interestingly, we show here a positive correlation between Δ40p53 and netrin-1 gene expression in melanoma and colorectal cancer cohorts. Moreover, netrin-1 and its dependence receptors are involved in melanoma and colorectal cancer progression (9,

49, 53, 54). Our data thus suggest for the first time a FLp53-independent pro-tumoral role for Δ40p53, owing to its ability to transactivate an anti-apoptotic protein such as netrin-1.

Regulation of netrin-1 and UNC5B receptor by the Δ40p53 isoform could have significant therapeutic consequences. Indeed, the fact that both the ligand and its dependence receptor are up-regulated in human cancers co-expressing Δ40p53 could enhance dependency of tumor cell survival on netrin-1 expression. Specifically, inhibition of interference of netrin-1 in these cancer cells should lead to dependence receptor-induced apoptosis and tumor regression. Our results demonstrate that silencing of netrin-1 expression by RNA interference induces cell death only in cells that are forced to produce Δ40p53 and consequently express high levels of netrin-1 and UNC5B. From a therapeutic point of view, we show here that, upon induction of Δ40p53, interference of the binding between netrin-1 and UNC5B with an anti-netrin-1 neutralizing antibody is sufficient to inhibit tumor growth in two different preclinical models of chicken CAM and *nude* mice.

In conclusion, we show here for the first time that the Δ40p53 isoform could positively regulate an anti-apoptotic protein, such as netrin-1, in a FLp53-independent way. In addition, this regulation of Δ40p53 could explain the increased transcript level of this survival protein, observed in several human cancers. Indeed, each mutation changing the ratio between FLp53 and Δ40p53 generation (*i.e.*, non-sense mutations in exon 2/3) could confer a selective advantage to cancer cells. Δ40p53 could inhibit the tumor suppressor activity of FLp53, acting as a dominant-negative protein, but could also actively transactivate pro-tumoral factors, such as shown here for netrin-1. In this context, a promising therapeutic strategy could be to inhibit the pro-tumoral activity, as we propose for netrin-1, instead of targeting the dominant-negative function of Δ40p53.

## Materials and Methods

### Generation of stable cell lines, reagents and transfection procedures

A549 and H1299 cell lines were obtained from the ATCC (Manassas, VA, USA). hTERT and cdk4-immortalized LHCN-M2 cells were a kind gift from Dr Vincent Mouly, (Center for research In Myology, Paris, France) (55). HCT116$^{p53-/-}$ cells were generated previously (42) and were kindly provided by B. Vogelstein (Ludwig Center at Johns Hopkins, Baltimore, MD). N-terminal HA-tagged human FLp53, ∆40p53 and ∆133p53 coding sequences were cloned at SfiI sites in the pITR plasmid (56). Detailed cell culture conditions, reagents, transfection procedures, and protocols for generation of stable cell lines are provided in *SI Appendix*, Supplementary Materials and Methods. siRNA and small guide cloning sequences are listed in *SI Appendix*, Fig. S7.

### Quantitative RT-PCR and western blot analysis

Total RNAs were extracted using the NucleoSpin® RNA Plus Kit (Macherey Nagel, Düren, Germany) according to the manufacturer's protocol. RT-PCR reactions were performed with the PrimeScript RT Reagent Kit (Takara Bio Europe, Saint-Germain-en-Laye, France). For immunoblotting analysis, cells were lysed by sonication in SDS buffer (10 mM Tris-HCl pH 7.4, 10% glycerol, 5% SDS, 1% TX-100, 100 mM DTT) in the presence of protease inhibitor cocktail (Roche Applied Science). Antibodies and detailed protocols are supplied in *SI Appendix*, Supplementary Materials and Methods. Primer sequences are available in *SI Appendix*, Fig. S7.

### Reporter assay and chromatin immunoprecipitation assay

Stable A549 cells inducible for FLp53 or Δ40p53 were plated in 12-well plates and transfected with the different firefly luciferase reporters containing wild-type or p53-mutated netrin-1 promoter constructs, described before (1, 9, 39) (*SI Appendix*, Supplementary Materials and Methods). Chromatin immunoprecipitation assay was performed as previously described (1), with some minor changes, described in *SI Appendix*, Supplementary Materials and Methods. Sequences of primers used for ChIP analysis are illustrated in *SI Appendix*, Fig. S7.

**Cell Death Assays**

For DNA fragmentation analysis (SubG1), DNA content was evaluated using the NucleoCounter NC-3000 system (ChemoMetec A/S, Allerød, Denmark). For AnnexinV and propidium iodide (PI) double staining, Annexin V positive cells were then evaluated by fluorescence activated cell sorting (FACS) on FACSCanto II (BD Biosciences, San Jose, CA, USA). Caspase-3 activity assay was performed as described previously (56). Detailed protocols are available on *SI Appendix*, Supplementary Materials and Methods.

**Xenografts *in ovo* and in *nude* mice**

For chick chorioallantoic membrane (CAM) assay, cells were seeded on 10 days-old CAMs, together with netrin-1 neutralizing antibody NP137 and relative control NP001 (10 μg/mL) (Netris Pharma, Lyon, France) and doxycycline (2 μg/mL). For xenografts in *nude* mice, A549 cells were implanted in 5-week-old female athymic *nude* Foxn1$^{nu/nu}$ mice. Procedures and treatment administration are detailed in *SI Appendix*, Supplementary Materials and Methods.

All experiments were performed in accordance with relevant guidelines and regulations of animal ethics committee (Authorization APAFIS n°: 28723; accreditation of laboratory animal care by CECCAP, ENS Lyon-PBES, France).

**Patients and tumor samples**

24 melanoma samples were collected as previously described (54), whereas 19 primary colorectal cancer tissue samples were obtained from the Biological Resource Centre (CRB, Centre de Resource Biologique) of Léon Bérard Centre (protocol number: BB-0033-00050) (Lyon, France), as previously described (57) (*SI Appendix*, Supplementary Materials and Methods).

## Acknowledgements

We wish to thank Brigitte Manship for critical reading of the manuscript, Dr Jean-Christophe Bourdon for p53-related materials and Nicolas Gadot (Plateforme Anatomopathologie Recherche, Université de Lyon, Université Claude Bernard Lyon 1, INSERM 1052, CNRS 5286, Centre Léon Bérard, Centre de recherche en Cancérologie de Lyon (CRCL), Lyon, 69373, France) for histological examination. This work was supported by institutional grants from CNRS, INSERM, University of Lyon, Centre Léon Bérard and from the Ligue Contre le Cancer, INCA, ANR, ERC and Fondation Bettencourt. Yan Sun and Hong Wang have been supported by a fellowship from China Scholarship Council, Ambroise Manceau and Lisa Frydman from Ligue Contre le Cancer, Valeria Basso from Nuovo-Soldati Cancer Research Foundation.

## Authors Contribution

Investigation, Y.S., A.M., L.F., L.C., D.N., V.B., H.W. and A.P.; Conceptualization, Y.S., P.M. and A.P.; Resources, L.C. and C.M.; Supervision, J.F., C.M., P.M. and A.P.; Writing – Original Draft, P.M. and A.P.; Writing –Review & Editing, P.M. and A.P.; Funding Acquisition, P.M.

## Conflict of Interest

P.M. and D.N. declare to have conflict of interest as respectively shareholder and employee of Netris Pharma. The other authors declare that they have no conflict of interest.

## References


1. A. Paradisi *et al.*, Combining chemotherapeutic agents and netrin-1 interference potentiates cancer cell death. *EMBO molecular medicine* **5**, 1821-1834 (2013).
2. M. Grandin *et al.*, Structural Decoding of the Netrin-1/UNC5 Interaction and its Therapeutical Implications in Cancers. *Cancer cell* **29**, 173-185 (2016).
3. P. Mehlen, D. E. Bredesen, Dependence receptors: from basic research to drug development. *Science signaling* **4**, mr2 (2011).
4. P. Mehlen, C. Delloye-Bourgeois, A. Chedotal, Novel roles for Slits and netrins: axon guidance cues as anticancer targets? *Nature reviews. Cancer* **11**, 188-197 (2011).
5. D. Goldschneider, P. Mehlen, Dependence receptors: a new paradigm in cell signaling and cancer therapy. *Oncogene* **29**, 1865-1882 (2010).
6. A. Paradisi, P. Mehlen, Netrin-1, a missing link between chronic inflammation and tumor progression. *Cell cycle* **9**, 1253-1262 (2010).
7. P. Mehlen, A. Puisieux, Metastasis: a question of life or death. *Nature reviews. Cancer* **6**, 449-458 (2006).
8. J. Fitamant *et al.*, Netrin-1 expression confers a selective advantage for tumor cell survival in metastatic breast cancer. *Proceedings of the National Academy of Sciences of the United States of America* **105**, 4850-4855 (2008).
9. A. Paradisi *et al.*, NF-kappaB regulates netrin-1 expression and affects the conditional tumor suppressive activity of the netrin-1 receptors. *Gastroenterology* **135**, 1248-1257 (2008).
10. C. Delloye-Bourgeois *et al.*, Netrin-1 acts as a survival factor for aggressive neuroblastoma. *The Journal of experimental medicine* **206**, 833-847 (2009).
11. C. Delloye-Bourgeois *et al.*, Interference with netrin-1 and tumor cell death in non-small cell lung cancer. *Journal of the National Cancer Institute* **101**, 237-247 (2009).

12. A. Paradisi *et al.*, Netrin-1 up-regulation in inflammatory bowel diseases is required for colorectal cancer progression. *Proceedings of the National Academy of Sciences of the United States of America* **106**, 17146-17151 (2009).

13. K. H. Vousden, C. Prives, Blinded by the Light: The Growing Complexity of p53. *Cell* **137**, 413-431 (2009).

14. U. M. Moll, S. Wolff, D. Speidel, W. Deppert, Transcription-independent pro-apoptotic functions of p53. *Curr Opin Cell Biol* **17**, 631-636 (2005).

15. D. R. Green, G. Kroemer, Cytoplasmic functions of the tumour suppressor p53. *Nature* **458**, 1127-1130 (2009).

16. R. Candau *et al.*, Two tandem and independent sub-activation domains in the amino terminus of p53 require the adaptor complex for activity. *Oncogene* **15**, 807-816 (1997).

17. C. A. Brady *et al.*, Distinct p53 transcriptional programs dictate acute DNA-damage responses and tumor suppression. *Cell* **145**, 571-583 (2011).

18. K. D. Sullivan, M. D. Galbraith, Z. Andrysik, J. M. Espinosa, Mechanisms of transcriptional regulation by p53. *Cell death and differentiation* **25**, 133-143 (2018).

19. J. C. Bourdon *et al.*, p53 isoforms can regulate p53 transcriptional activity. *Genes & development* **19**, 2122-2137 (2005).

20. V. Marcel *et al.*, Biological functions of p53 isoforms through evolution: lessons from animal and cellular models. *Cell death and differentiation* **18**, 1815-1824 (2011).

21. M. P. Khoury, J. C. Bourdon, The isoforms of the p53 protein. *Cold Spring Harbor perspectives in biology* **2**, a000927 (2010).

22. V. Marcel, P. Hainaut, p53 isoforms - a conspiracy to kidnap p53 tumor suppressor activity? *Cellular and molecular life sciences : CMLS* **66**, 391-406 (2009).

23. A. Ghosh, D. Stewart, G. Matlashewski, Regulation of human p53 activity and cell localization by alternative splicing. *Molecular and cellular biology* **24**, 7987-7997 (2004).

24. S. Courtois *et al.*, DeltaN-p53, a natural isoform of p53 lacking the first transactivation domain, counteracts growth suppression by wild-type p53. *Oncogene* **21**, 6722-6728 (2002).

25. G. Matlashewski, D. Pim, L. Banks, L. Crawford, Alternative splicing of human p53 transcripts. *Oncogene Res* **1**, 77-85 (1987).

26. V. Marcel *et al.*, p53 regulates the transcription of its Delta133p53 isoform through specific response elements contained within the TP53 P2 internal promoter. *Oncogene* **29**, 2691-2700 (2010).

27. J. Lin, J. Chen, B. Elenbaas, A. J. Levine, Several hydrophobic amino acids in the p53 amino-terminal domain are required for transcriptional activation, binding to mdm-2 and the adenovirus 5 E1B 55-kD protein. *Genes & development* **8**, 1235-1246 (1994).

28. S. W. Chi *et al.*, Structural details on mdm2-p53 interaction. *The Journal of biological chemistry* **280**, 38795-38802 (2005).

29. R. Takahashi, S. N. Markovic, H. J. Scrable, Dominant effects of Delta40p53 on p53 function and melanoma cell fate. *The Journal of investigative dermatology* **134**, 791-800 (2014).

30. H. Hafsi, D. Santos-Silva, S. Courtois-Cox, P. Hainaut, Effects of Delta40p53, an isoform of p53 lacking the N-terminus, on transactivation capacity of the tumor suppressor protein p53. *BMC cancer* **13**, 134 (2013).

31. I. Horikawa *et al.*, Delta133p53 represses p53-inducible senescence genes and enhances the generation of human induced pluripotent stem cells. *Cell death and differentiation* **24**, 1017-1028 (2017).

32. Y. Yin, C. W. Stephen, M. G. Luciani, R. Fahraeus, p53 Stability and activity is regulated by Mdm2-mediated induction of alternative p53 translation products. *Nature cell biology* **4**, 462-467 (2002).

33. M. M. Candeias *et al.*, Expression of p53 and p53/47 are controlled by alternative mechanisms of messenger RNA translation initiation. *Oncogene* **25**, 6936-6947 (2006).

34. D. J. Powell *et al.*, Stress-dependent changes in the properties of p53 complexes by the alternative translation product p53/47. *Cell cycle* **7**, 950-959 (2008).

35. P. I. Thakore *et al.*, Highly specific epigenome editing by CRISPR-Cas9 repressors for silencing of distal regulatory elements. *Nature methods* **12**, 1143-1149 (2015).

36. L. A. Gilbert *et al.*, CRISPR-mediated modular RNA-guided regulation of transcription in eukaryotes. *Cell* **154**, 442-451 (2013).

37. M. Adli, The CRISPR tool kit for genome editing and beyond. *Nature communications* **9**, 1911 (2018).

38. R. Urrutia, KRAB-containing zinc-finger repressor proteins. *Genome biology* **4**, 231 (2003).

39. C. Delloye-Bourgeois *et al.*, Nucleolar localization of a netrin-1 isoform enhances tumor cell proliferation. *Science signaling* **5**, ra57 (2012).

40. M. Ménard *et al.*, Hey1- and p53-dependent TrkC proapoptotic activity controls neuroblastoma growth. *PLoS biology* **16**, e2002912 (2018).

41. A. L. Genevois *et al.*, Dependence receptor TrkC is a putative colon cancer tumor suppressor. *Proceedings of the National Academy of Sciences of the United States of America* **110**, 3017-3022 (2013).

42. F. Bunz *et al.*, Requirement for p53 and p21 to sustain G2 arrest after DNA damage. *Science* **282**, 1497-1501 (1998).

43. G. Hofstetter *et al.*, The N-terminally truncated p53 isoform Delta40p53 influences prognosis in mucinous ovarian cancer. *International journal of gynecological cancer : official journal of the International Gynecological Cancer Society* **22**, 372-379 (2012).

44. K. A. Avery-Kiejda *et al.*, Small molecular weight variants of p53 are expressed in human melanoma cells and are induced by the DNA-damaging agent cisplatin. *Clinical cancer research : an official journal of the American Association for Cancer Research* **14**, 1659-1668 (2008).

45. K. A. Avery-Kiejda, B. Morten, M. W. Wong-Brown, A. Mathe, R. J. Scott, The relative mRNA expression of p53 isoforms in breast cancer is associated with clinical features and outcome. *Carcinogenesis* **35**, 586-596 (2014).

46. L. Mazelin *et al.*, Netrin-1 controls colorectal tumorigenesis by regulating apoptosis. *Nature* **431**, 80-84 (2004).

47. F. Llambi, F. Causeret, E. Bloch-Gallego, P. Mehlen, Netrin-1 acts as a survival factor via its receptors UNC5H and DCC. *The EMBO journal* **20**, 2715-2722 (2001).

48. P. Mehlen *et al.*, The DCC gene product induces apoptosis by a mechanism requiring receptor proteolysis. *Nature* **395**, 801-804 (1998).

49. M. Castets *et al.*, DCC constrains tumour progression via its dependence receptor activity. *Nature* **482**, 534-537 (2011).

50. F. Mille *et al.*, Interfering with multimerization of netrin-1 receptors triggers tumor cell death. *Cell death and differentiation* **16**, 1344-1351 (2009).

51. T. Anbarasan, J. C. Bourdon, The Emerging Landscape of p53 Isoforms in Physiology, Cancer and Degenerative Diseases. *International journal of molecular sciences* **20** (2019).

52. M. Vieler, S. Sanyal, p53 Isoforms and Their Implications in Cancer. *Cancers* **10** (2018).

53. A. Bernet *et al.*, Inactivation of the UNC5C Netrin-1 receptor is associated with tumor progression in colorectal malignancies. *Gastroenterology* **133**, 1840-1848 (2007).

54. A. Boussouar *et al.*, Netrin-1 and Its Receptor DCC Are Causally Implicated in Melanoma Progression. *Cancer research* **80**, 747-756 (2020).

55. C. H. Zhu *et al.*, Cellular senescence in human myoblasts is overcome by human telomerase reverse transcriptase and cyclin-dependent kinase 4: consequences in aging muscle and therapeutic strategies for muscular dystrophies. *Aging cell* **6**, 515-523 (2007).

56. H. Wang *et al.*, The Proto-oncogene c-Kit Inhibits Tumor Growth by Behaving as a Dependence Receptor. *Molecular cell* **72**, 413-425 e415 (2018).

57. F. Di Ruocco *et al.*, Alu RNA accumulation induces epithelial-to-mesenchymal transition by modulating miR-566 and is associated with cancer progression. *Oncogene* **37**, 627-637 (2018).

58. K. F. Macleod *et al.*, p53-dependent and independent expression of p21 during cell growth, differentiation, and DNA damage. *Genes & development* **9**, 935-944 (1995).

## Figure Legends

**Fig. 1.** Netrin-1 regulation by p53 requires the transcriptional activity of the TAD2 domain. (A) Schematic representation of the structure of p53 domains. The structure can be divided into three components: an N-terminal domain, encompassing two distinct transactivation domains (TAD1 and TAD2) and a proline-rich domain (PXXP); a core domain with the DNA-binding domain, accounting for binding to responsive elements in a promoter; a C-terminal domain, containing an oligomerization domain, allowing p53 tetramerization, and a basic domain required for protein stability. TAD1- or TAD2-inactivating p53 mutated proteins are indicated in red. (B, C) TAD2 mutant p53 proteins are unable to trigger netrin-1. Stable H1299 cell lines, inducible for wild-type or mutant p53 proteins, were treated with doxycycline for 24 h and expression of netrin-1, p21 and p53 was analyzed by Western blot (B) or quantitative RT-PCR (C). The glyceraldehyde 3-phosphate dehydrogenase (GAPDH) protein was used to normalize Western blots, while quantitative RT-PCR was normalized using TATA binding protein (TBP) and β-glucuronidase (GUSB) as housekeeping genes. Immunoblots presented in B are representative of three independent experiments. Data in C are presented as mean ± SEM (n = 3). *, $p < 0.05$; **, $p < 0.01$; ***, $p < 0.001$; ****, $p < 0.0001$. NT, not treated; Dox, doxycycline; NTN1, netrin-1; A.U., arbitrary units.

**Fig. 2.** Δ40p53, but not Δ133p53, regulates netrin-1 and UNC5B expression. (A) Schematic representation of the structure of p53 isoform domains. The Δ40p53 isoform

lacks TAD1 (in yellow), while Δ133p53 lacks the entire N-terminal domain (including TAD1, TAD2 and PXXP domains) and a small part of DNA-binding domain (in dark blue). (B, C) Over-expression of Δ40p53 is sufficient to induce netrin-1 gene expression. Stable A549 cell lines, inducible for empty vector (pITR), Δ40p53α-HA and Δ133p53α-HA, were treated with doxycycline for 24 h. Netrin-1, UNC5B and p21 gene expression was analyzed by quantitative RT-PCR (B), while protein expression of netrin-1, p21 and BAX was evaluated by Western blot (C). Expression of HA-tagged p53 isoforms was also assessed by Western blot. (D) Δ40p53-dependent netrin-1 induction requires Δ40p53 transcriptional activity. Stable A549 cell lines, inducible for wild-type or TAD-mutated ($\Delta 40p53^{14,15}$) Δ40p53 protein, were treated with doxycycline. Netrin-1, p21 and p53 protein expression was evaluated by Western blot. Ku80 protein was used to normalize protein expression. (E) Δ40p53 expression, but not Δ133p53, increases doxorubicin-induced netrin-1 up-regulation, while it decreases p21 gene expression upon doxorubicin treatment. Stable A549 cells inducible for Δ40p53 or Δ133p53 were treated with doxycycline and/or doxorubicin for 24 h. Expression levels of netrin-1 (NTN1), UNC5B and p21 were evaluated by quantitative RT-PCR. Expression of TBP and GUSB was used as housekeeping genes. Immunoblots in C and D are representative of three independent experiments. Data in B and E are presented as mean ± SEM (n = 3). *, $p < 0.05$; **, $p < 0.01$; ***, $p < 0.001$; ****, $p < 0.0001$. NT, not treated; Dox, doxycycline; NTN1, netrin-1; HA, influenza hemagglutinin; DoxoR, doxorubicin; CTRL, control; A.U., arbitrary units. OD, oligomerization domain; BD, basic domain.

**Fig. 3.** Full-length p53 is not necessary for netrin-1 regulation by Δ40p53. (A, B) Over-expression of full-length p53 or Δ40p53 in p53-null cells is sufficient to induce netrin-1 expression. Stable p53-null H1299 cell lines, inducible for full-length p53 (p53FL) or Δ40p53 proteins, alone or in combination (p53FL+Δ40p53), were treated with doxycycline for 24 h. Netrin-1 (NTN1) gene expression was assessed by quantitative RT-PCR (n = 3) (A). Protein levels of netrin-1 and p21, as well as p53FL and Δ40p53, were evaluated by Western blot (B). (C, D) Silencing endogenous p53 expression does not affect Δ40p53-dependent netrin-1 up-regulation. Stable A549 cell lines, inducible for Δ40p53, were transfected with a scramble siRNA (siCTRL) or with a specific siRNA targeting exon 2 of p53 gene (sip53). 24 hours after transfection, cells were treated with doxorubicin or doxycycline for a further 24 h, and netrin-1 (NTN1) protein and transcript levels were measured by Western blot (C) and quantitative RT-PCR (n = 6) (D), respectively. Expression of endogenous FLp53 and over-expressed Δ40p53α was also evaluated by Western blot, using Pab 1801 p53 antibody (C). (E) Δ40p53-induced netrin-1 gene expression is not altered by knocking-down endogenous p53. A549 cells were infected using CRISPR/Cas9-modified pLV-hU6-sgRNA-hUbC-dCas9-KRAB-T2a-Puro plasmid, and stable cell lines were generated using firefly luciferase-control (sgLUC) or p53-specific (sgp53A and sgp53B) small guide RNAs. Endogenous p53-repressed cell lines were then transfected with empty (pITR) or Δ40p53 sleeping-beauty plasmids. Stable A549 cell lines knockdown for p53 and inducible for Δ40p53 were treated with doxorubicin and doxycycline for 24 h. Efficacy of endogenous p53 repression was evaluated by Western blot, using p53-DO1 antibody, while anti-HA-tagged antibody provided data on Δ40p53 expression. In addition, netrin-1 and p21 protein levels were assessed by Western

blot. Immunoblots in B, C and E are representative of three independent experiments. Quantitative PCR results in A and D are presented as mean ± SEM. ns, non-significant; **, $p < 0.01$; ***, $p < 0.001$; ****, $p < 0.0001$. NT, not treated; Dox, doxycycline; DoxoR, doxorubicin; NTN1, netrin-1; HA, influenza hemagglutinin; sg, small guide; FLp53, full-length p53; sgLUC, small guide targeting luciferase.

**Fig. 4.** Δ40p53 directly binds to and activates the netrin-1 promoter. (A) Δ40p53 activates the netrin-1 promoter, binding to canonical p53 responsive elements. Stable H1299 cells inducible for Δ40p53 or full-length p53 (FLp53) were transfected with wild-type (NetP) or mutated for p53 binding site (NetP mut) promoters, as well as for the p21 promoter (p21P). 24 h after transfection, cells were treated with 2 μg/mL of doxycycline for a further 24 h and promoter activities were assessed by luciferase assay. Values represent mean ± SEM (n = 3). Induction of Δ40p53 and FLp53 was verified by Western blot, using α-HA antibody. (B) Δ40p53 directly binds to the netrin-1 promoter. Stable H1299 cells inducible for Δ40p53-HA were treated with 2 μg/mL of doxycycline for 24 h. Chromatin immunoprecipitation (ChIP) was performed using α-HA antibody, as described in the Material and Methods section. Δ40p53-co-precipitated DNA was analyzed by quantitative PCR, using two different primer couples surrounding the p53 binding site in the netrin-1 promoter (p53RE-1 and -2) (1). A couple of primers, amplifying a not-p53-related fragment in the netrin-1 promoter, was used as negative control (Neg CTRL). p21 primers, surrounding the p53 binding site -1354 contained in the p21 promoter (58), were used to confirm activation and binding of p21 promoter upon Δ40p53 induction. Values represent mean ± SEM (n = 4). Western blot in the inset, performed with α-HA antibody, confirmed

Δ40p53 expression in immunoprecipitated samples. **, p < 0.01; ***, p < 0.001; ****, p < 0.0001; ns, non-significant. CTRL, control; Dox, doxycycline; FLp53, full-length p53; NetP, netrin-1 promoter; p21P, p21 promoter.

**Fig. 5.** Endogenous Δ40p53 regulates netrin-1 expression. (A) Schematic representation of the 5' sequence of p53 gene. ATG codons for full-length p53 (ATG1) and Δ40p53 (ATG40) are indicated, as well as two small guide RNAs (sgRNAs), designed near ATG1 (sgFLp53) and ATG40 (sgTOTp53). In insets, sequences of sgRNAs are displayed in blue, while ATG codons are in red. (B, C) Forced endogenous Δ40p53 expression drives an increase in netrin-1 and UNC5B. Stable LHCN-M2 cells knocked out for the p53 gene were generated using firefly luciferase-control (sgLUC), ATG1- (sgFLp53) or ATG40- (sgTOTp53) targeting sgRNAs. Western blot analysis, using the pan-p53 antibodies DO-11 and Pab 1801, confirmed the complete knockout of all isoforms of p53 in LHCN-M2 cells generated with guide sgTOTp53, targeting Δ40p53 ATG40 codon, while guide sgFLp53, targeting only the ATG1 codon of full-length p53 forced cells to produce a shorter p53 isoform, instead of full-length p53, with a molecular weight corresponding to Δ40p53 (B). Western blot with the N-terminal p53-DO-1 antibody confirmed that this band corresponds to a p53 isoform lacking the very first N-terminal amino acids. Netrin-1, UNC5B and Ku80 protein levels, revealed by Western blot, are also displayed. Expression levels of netrin-1 (NTN1), UNC5B and p21 transcripts were analyzed by quantitative RT-PCR (C). Immunoblots in B are representative of three independent experiments. Quantitative PCR results in C are presented as mean ± SEM (n = 3). ns, non-significant;

*, $p < 0.05$; **, $p < 0.01$; ***, $p < 0.001$; Ex, exon; MW, molecular weight; KDa, Kilodalton; NTN1, netrin-1.

**Fig. 6.** Δ40p53 expression sensitizes cells to netrin-1 silencing-induced apoptosis. (A, B, C) Parental or stable LHCN-M2 cells, infected with control (sgLUC), FLp53/Δ40p53 (sgTOTp53) or FLp53 only (sgFLp53) knock-out lentiviral constructs, were transfected with scramble (siCTRL) or netrin-1-specific (siNet) siRNAs. Induction of apoptosis was evaluated by DNA fragmentation assay (SubG1) (A), caspase-3 activity (B) or Annexin V and PI double staining analyzed by flow cytometry (C). A representative DNA fragmentation experiment is shown in the right part of panel (A). (C) Stable A549 cells, inducible for Δ40p53, were transfected with siCTRL or siNet siRNAs. 24 hours after transfection, cells were treated with 2 µg/mL of doxycycline and induction of apoptosis was evaluated 72 h later by DNA fragmentation assay. Results are presented as mean ± SEM (n = 3). ns, non-significant; **, $p < 0.01$; ****, $p < 0.0001$; Dox, doxycycline; sg, small guide.

**Fig. 7.** Δ40p53 expression sensitizes cells to netrin-1 interference-induced tumor growth inhibition. (A) Schematic representation of the experimental settings of tumor growth in the chicken chorioallantoic membrane (CAM) model. A549 cells were seeded in the CAM of E10 chick embryo, together with doxycycline and Netrin-1 neutralizing antibody. (B) Weight and size of CAM-engrafted tumors. Primary tumors were treated with 10 µg/mL of neutralizing anti-netrin-1 antibody (NP137) or isotypic control (Iso-mAb), in presence of 2 µg/mL of doxycycline. After seven days, primary tumors were imaged using Zeiss

Microscope and tumor areas were measured with AxioVision Rel Software. Moreover, tumors were resected and weighted. n indicated the number of samples for each condition. (C) Representative images of A549 primary tumors, treated with PBS or doxycycline (dox), in combination with anti-netrin-1 (NP137) or isotypic antibodies (Iso-mAb). Red lines represent tumor volume automatically measured by AxioVision Software (scale bar = 1 mm). (D) Neutralizing netrin-1 antibody (NP137) inhibits tumor growth in *nude* mice engrafted with stable A549 inducible for Δ40p53 and watered with doxycycline, compared to animals treated with isotypic antibody (Iso-mAb) (n = 10 for each group). Tumor volume were measured at the indicated days after the first treatment with antibodies. (E) Anti-tumoral effect of NP137 antibody is associated with apoptosis induction. Engrafted tumors were resected 36 days after beginning treatments and apoptosis was evaluated by immunohistochemical staining of active caspase-3. (F) Δ40p53 expression in colorectal cancer cells sensitizes cells to netrin-1 inhibition in the CAM model. Wild-type or FLp53-knockout HCT116 cells were seeded in the CAM of E10 chick embryo, together with 10 µg/mL of anti-netrin-1 (NP137) or control (Iso-mAb) antibodies. Tumors were imaged after seven days and tumor areas were measured, as well as their weight. n indicated the number of samples for each condition. Data are represented as mean ± SEM. ns, non-significant; *, $p < 0.05$; **, $p < 0.01$; ***, $p < 0.001$; ****, $p < 0.0001$; Dox, doxycycline; CAM, chorioallantoic membrane; mAb, monoclonal antibody; Iso, isotypic; cCaspase-3, cleaved caspase-3.

**Fig. 8.** Netrin-1 and Δ40p53 gene expression is correlated in human melanoma and colorectal tumor biopsies (A) Correlation between Δ40p53 and netrin-1 gene expression

in melanoma (n = 24) and colorectal cancer (n = 19) biopsies. mRNA levels of Δ40p53 was plotted as a function of netrin-1 (NTN1) expression, and the level of fit was obtained by calculating the coefficient of determination $R^2$. (B) Melanoma and colorectal cancer biopsies were separated according to their relative Δ40p53 gene expression, in order to form high (exceeding the median gene expression value) or low Δ40p53 expression groups. Netrin-1 gene expression was then evaluated in Δ40p53 expression groups. *, $p < 0.05$; NTN1, netrin-1; A.U., arbitrary units.

Figure 1

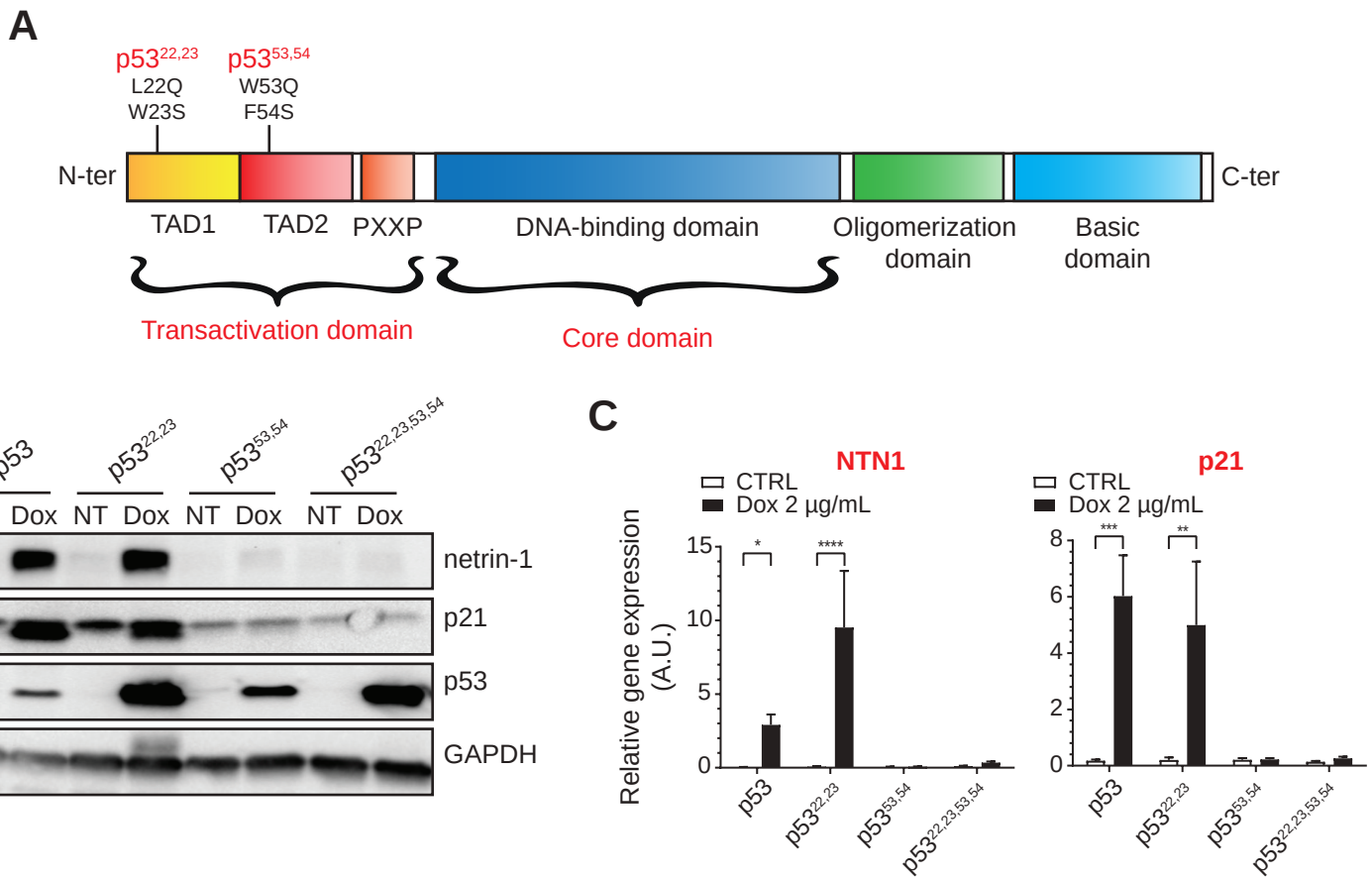
A
p53 22,23
L22Q
W23S
p53 53,54
W53Q
F54S
N-ter
C-ter
TAD1
TAD2
PXXP
DNA-binding domain
Oligomerization domain
Basic domain
Transactivation domain
Core domain


B
p53
p53 22,23
p53 53,54
p53 22,23,53,54
NT Dox NT Dox NT Dox NT Dox
netrin-1
p21
p53
GAPDH


C
NTN1
p21
CTRL
Dox 2 µg/mL
Relative gene expression (A.U.)
15
10
5
0
8
6
4
2
0
*
****
***
**
p53
p53 22,23
p53 53,54
p53 22,23,53,54

Figure 2

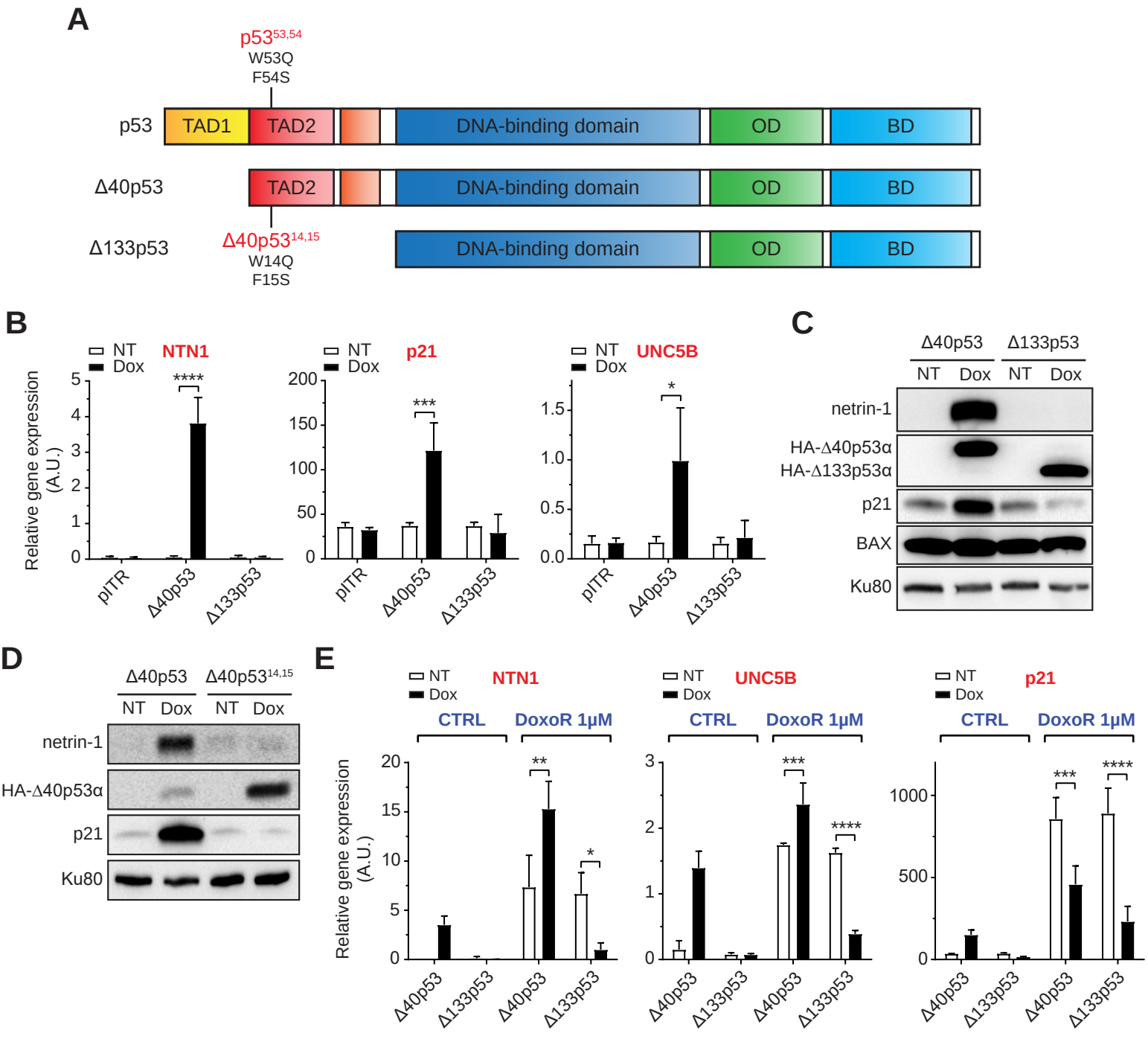
A
p53[53,54]
W53Q
F54S
p53
TAD1
TAD2
DNA-binding domain
OD
BD
Δ40p53
Δ133p53
Δ40p53[14,15]
W14Q
F15S
B
NT
Dox
NTN1
p21
UNC5B
Relative gene expression (A.U.)
pITR
Δ40p53
Δ133p53
C
Δ40p53
Δ133p53
netrin-1
HA-Δ40p53α
HA-Δ133p53α
p21
BAX
Ku80
D
Δ40p53
Δ40p53[14,15]
E
CTRL
DoxoR 1μM

Figure 3

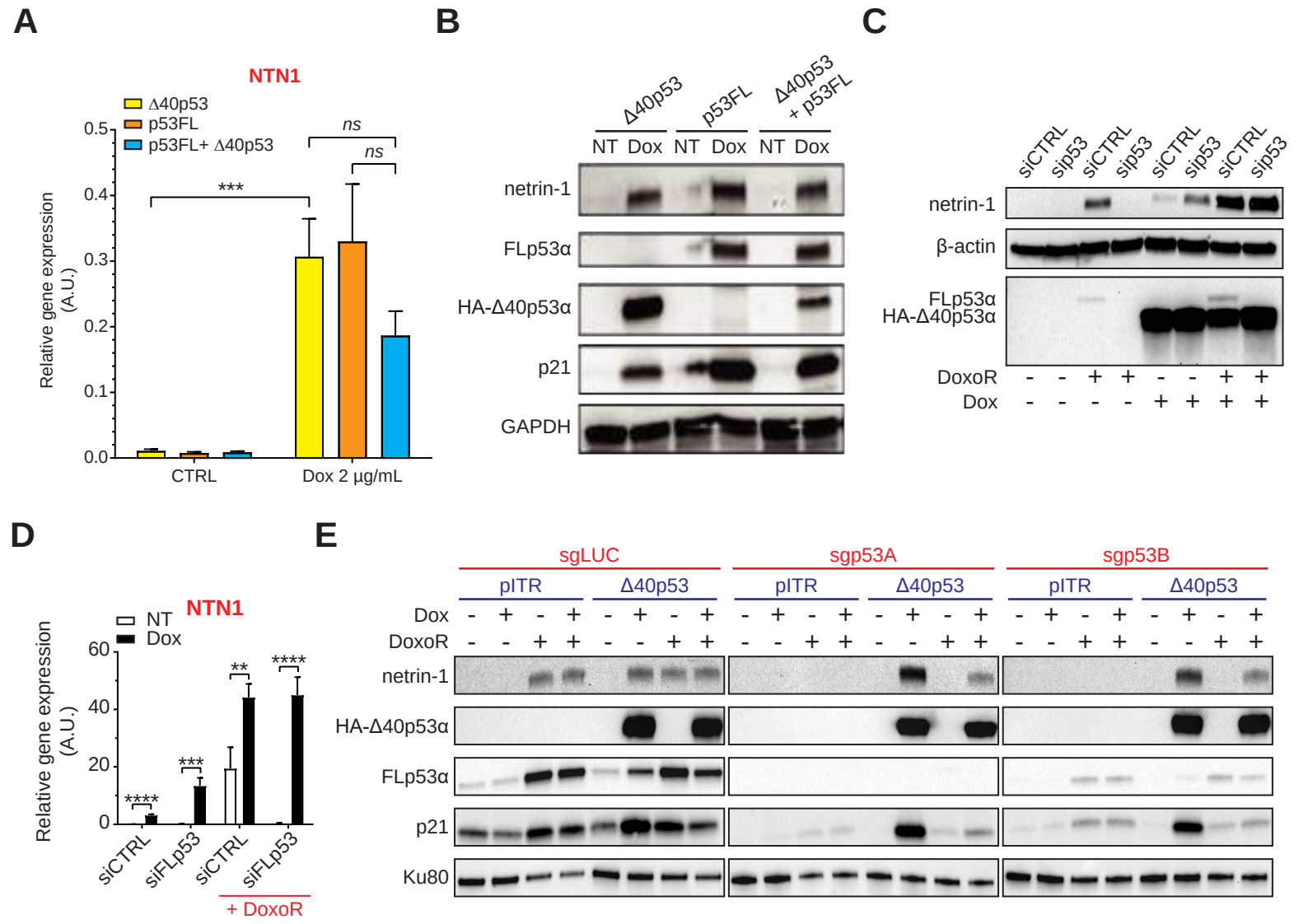
A
NTN1
Δ40p53
p53FL
p53FL+ Δ40p53
Relative gene expression (A.U.)
0.5
0.4
0.3
0.2
0.1
0.0
***
ns
ns
CTRL
Dox 2 µg/mL
B
Δ40p53
p53FL
Δ40p53 + p53FL
NT Dox NT Dox NT Dox
netrin-1
FLp53α
HA-Δ40p53α
p21
GAPDH
C
siCTRL sip53 siCTRL sip53 siCTRL sip53 siCTRL sip53
netrin-1
β-actin
FLp53α
HA-Δ40p53α
DoxoR - - + + - - + +
Dox - - - - + + + +
D
NTN1
NT
Dox
Relative gene expression (A.U.)
60
40
20
0
****
***
**
****
siCTRL
siFLp53
siCTRL
siFLp53
+ DoxoR
E
sgLUC
sgp53A
sgp53B
pITR
Δ40p53
Dox - + - + - + - + - + - + - + - + - + - + - +
DoxoR - - + + - - + + - - + + - - + + - - + + - - + +
netrin-1
HA-Δ40p53α
FLp53α
p21
Ku80

Figure 4

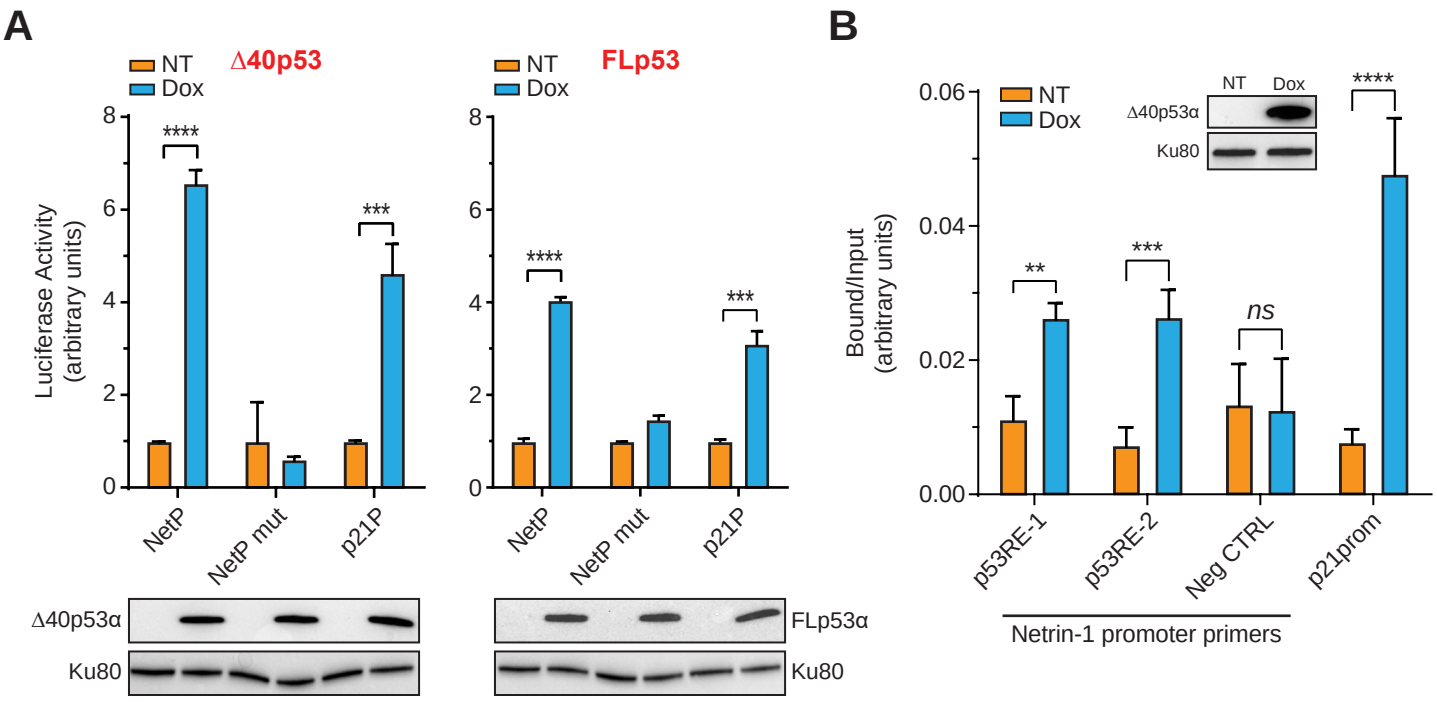
A
NT
Dox
Δ40p53
FLp53
Luciferase Activity (arbitrary units)
****
***
NetP
NetP mut
p21P
Δ40p53α
FLp53α
Ku80
B
Bound/Input (arbitrary units)
**
ns
p53RE-1
p53RE-2
Neg CTRL
p21prom
Netrin-1 promoter primers

Figure 5

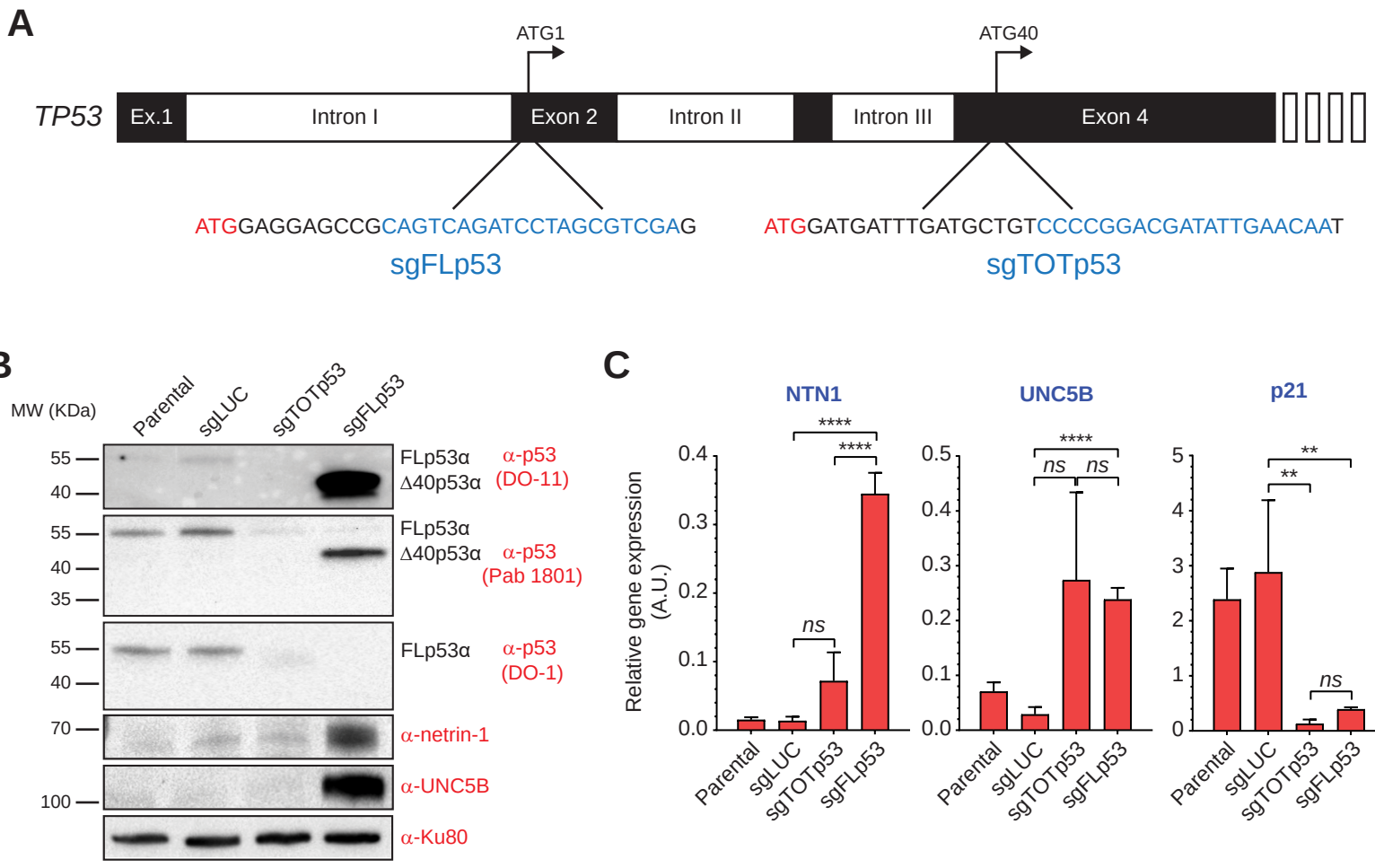
A
ATG1
ATG40
TP53
Ex.1
Intron I
Exon 2
Intron II
Intron III
Exon 4
ATGGAGGAGCCGCAGTCAGATCCTAGCGTCGAG
sgFLp53
ATGGATGATTTGATGCTGTCCCCGGACGATATTGAACAAT
sgTOTp53
B
MW (KDa)
Parental
sgLUC
sgTOTp53
sgFLp53
55
40
55
40
35
55
40
70
100
FLp53α
Δ40p53α
α-p53
(DO-11)
FLp53α
Δ40p53α
α-p53
(Pab 1801)
FLp53α
α-p53
(DO-1)
α-netrin-1
α-UNC5B
α-Ku80
C
NTN1
UNC5B
p21
Relative gene expression
(A.U.)
0.4
0.3
0.2
0.1
0.0
0.5
0.4
0.3
0.2
0.1
0.0
5
4
3
2
1
0
****
****
ns
****
ns
ns
**
**
ns
Parental
sgLUC
sgTOTp53
sgFLp53

Figure 6

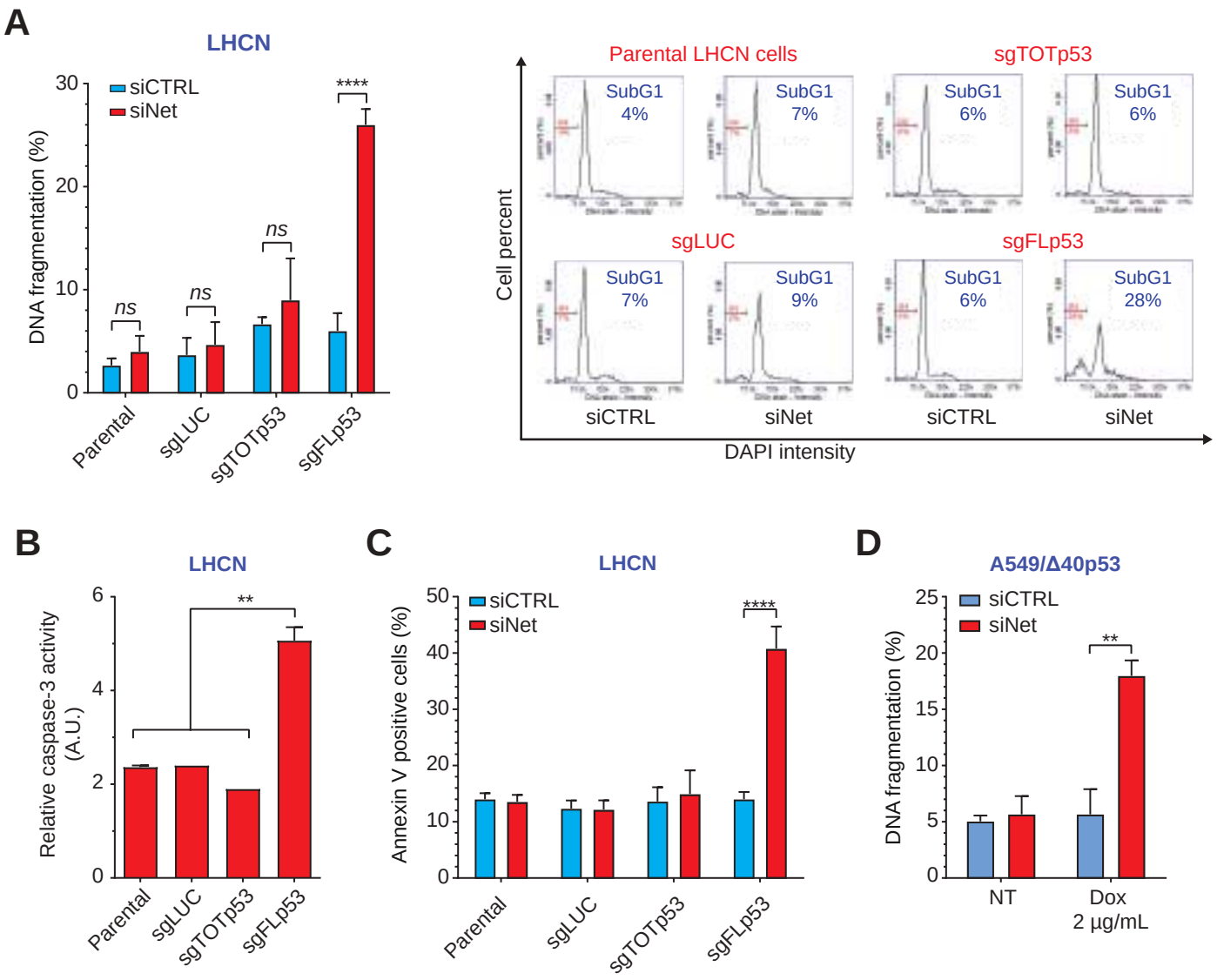
A
LHCN
siCTRL
siNet
DNA fragmentation (%)
30
20
10
0
ns
ns
ns
****
Parental
sgLUC
sgTOTp53
sgFLp53
Parental LHCN cells
sgTOTp53
sgLUC
sgFLp53
SubG1 4%
SubG1 7%
SubG1 6%
SubG1 6%
SubG1 7%
SubG1 9%
SubG1 6%
SubG1 28%
Cell percent
siCTRL
siNet
siCTRL
siNet
DAPI intensity
B
LHCN
Relative caspase-3 activity (A.U.)
6
4
2
0
**
Parental
sgLUC
sgTOTp53
sgFLp53
C
LHCN
siCTRL
siNet
Annexin V positive cells (%)
50
40
30
20
10
0
****
Parental
sgLUC
sgTOTp53
sgFLp53
D
A549/Δ40p53
siCTRL
siNet
DNA fragmentation (%)
25
20
15
10
5
0
**
NT
Dox
2 µg/mL

Figure 7

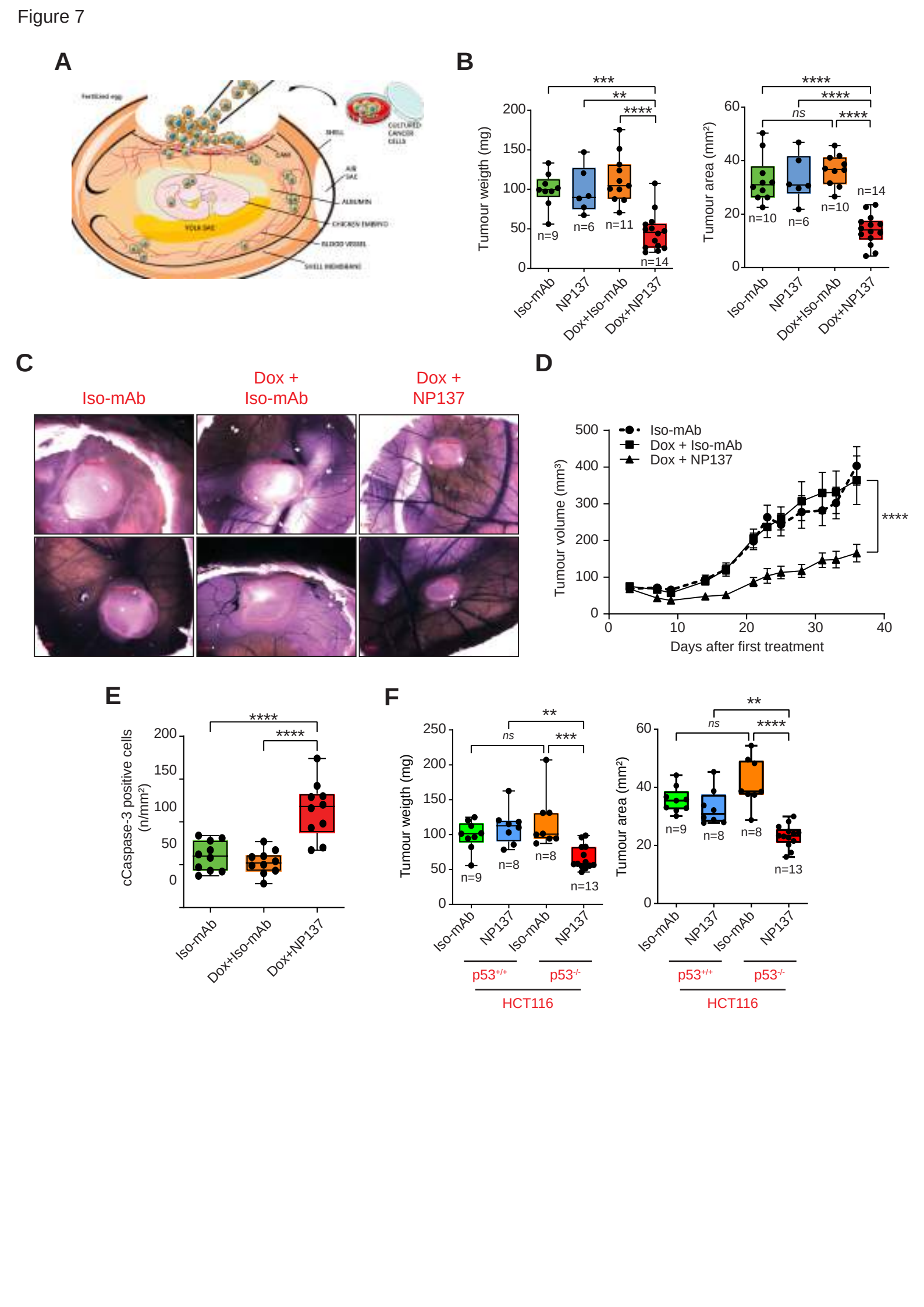
A
B
Tumour weigth (mg)
Tumour area (mm²)
Iso-mAb
NP137
Dox+Iso-mAb
Dox+NP137
n=9
n=6
n=11
n=14
n=10
n=6
n=10
n=14
C
Iso-mAb
Dox + Iso-mAb
Dox + NP137
D
Tumour volume (mm³)
Days after first treatment
E
cCaspase-3 positive cells (n/mm²)
F
p53+/+
p53-/-
HCT116

Figure 8

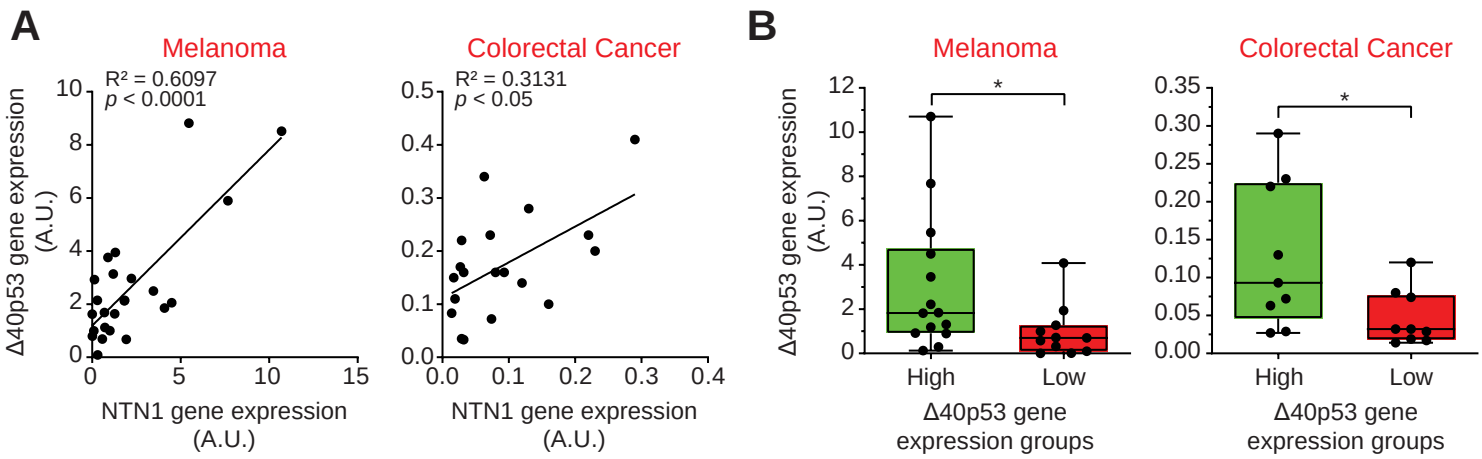
A
Melanoma
R² = 0.6097
p < 0.0001
Δ40p53 gene expression (A.U.)
NTN1 gene expression (A.U.)
Colorectal Cancer
R² = 0.3131
p < 0.05
NTN1 gene expression (A.U.)
B
Melanoma
Δ40p53 gene expression (A.U.)
High
Low
Δ40p53 gene expression groups
Colorectal Cancer
High
Low
Δ40p53 gene expression groups

PNAS
www.pnas.org

## Supplementary Information for

# Δ40p53 isoform up-regulates netrin-1/UNC5B expression and potentiates netrin-1 pro-oncogenic activity

Yan Sun[a], Ambroise Manceau[a,1], Lisa Frydman[a,1], Lucie Cappuccio[b], David Neves[c], Valeria Basso[a], Hong Wang[a], Joanna Fombonne[a], Carine Maisse[b], Patrick Mehlen[a,2], and Andrea Paradisi[a,2]

[a]Apoptosis, Cancer and Development Laboratory - Equipe labellisée 'La Ligue', LabEx DEVweCAN, Centre de Recherche en Cancérologie de Lyon, INSERM U1052-CNRS UMR5286, Université de Lyon, Université Claude Bernard Lyon1, Centre Léon Bérard, 69008 Lyon, France.

[b]IVPC UMR754 INRAE, Université de Lyon, Université Claude Bernard Lyon1, EPHE, Lyon, France.

[c]Netris Pharma, 69008 Lyon.

[1]A.M. and L.F. contributed equally to this work.

[2]To whom correspondence may be addressed. Email: andrea.paradisi@lyon.unicancer.fr or patrick.mehlen@lyon.unicancer.fr.

**This PDF file includes:**

## Supplementary Materials and Methods

### Cell Lines

Human lung A549 and colorectal HCT116 cancer cells were cultured in Dulbecco's modified Eagle's (DMEM) medium (Life Technologies, Carlsbad, CA, USA) containing 10% fetal bovine serum (Life Technologies) and 50 µg/mL gentamycin (Life Technologies). Human lung H1299 cancer cells were cultured in Roswell Park Memorial Institute (RPMI) 1640 + Glutamax medium (Life Technologies) containing 10% fetal bovine serum and 50 µg/mL gentamycin (Life Technologies). Human skeletal myoblasts LHCN-M2 were cultured in medium (four parts of DMEM medium to one part medium 199), supplemented with 20% fetal bovine serum (Life Technologies), 30 mM HEPES and 5 ng/mL HGF (R&D systems, Minneapolis, MN, USA), 1 µM dexamethasone (Sigma-Aldrich, Saint Quentin-Fallavier, France), 1.4 mg/L zinc sulphate (ZnSO4, Sigma-Aldrich) and 0.03 mg/L vitamin B12 (Sigma-Aldrich). All cell lines were regularly tested for mycoplasma contamination using the MycoAlert Mycoplasma Detection Kit (Lonza, Basel, Switzerland).

### Reagents and transfection procedures

Doxycycline hyclate and doxorubicin hydrochloride were obtained from Sigma-Aldrich. 21nt-siRNA were designed using the Designer of Small Interfering RNA (DSIR) tool (56), available on the http://biodev.extra.cea.fr/DSIR/DSIR.html site. siRNA oligonucleotides were synthetized by Sigma-Aldrich. siRNA transfection of LHCN-M2 was performed using lipofectamine RNAiMAX reagent (Life Technologies). For plasmid transfection to generate stable cell lines, A549 and H1299 cell lines were transfected using Jet Prime reagent (PolyPlus-Transfection, Illkirch, France). All

transfections were performed following the manufacturer's instructions. siRNA sequences are listed in *SI Appendix*, Fig. S7.

**Generation of stable cell lines**

For the generation of inducible stable cell lines, N-terminal HA-tagged human FLp53, Δ40p53 and Δ133p53 coding sequences were cloned at SfiI sites in the pITR plasmid, a sleeping beauty-based vector allowing the doxycycline inducible expression of p53 isoforms, as well as the constitutive expression of rtTA protein, puromycin resistance gene and green fluorescent protein (GFP), expressed under the control of the mouse phosphoglycerate kinase (PGK) promoter (1). Alternatively, p53 isoform sequences were cloned into the pITR2 plasmid, a modified version of the pITR vector, containing Zeocin resistance gene and mCherry fluorescent protein. A549 and H1299 cell lines were co-transfected with p53 isoform-pITR/pITR2 plasmid and a sleeping beauty transposase expression vector (SB100X). The pITR vector was a generous gift of Prof. Rolf Marschalek (Goethe-University of Frankfurt, Germany). Stable cell clones were selected for 3 days in puromycin-containing medium. Alternatively, stable cell lines were sorted by flow cytometry to selected GFP- or mCherry-positive cells. All the stable inducible cell lines were further tested for the expression of p53 isoforms in response to doxycycline. Plasmids containing cDNA sequence of FL53, Δ40p53 and Δ133p53 cDNA were a kind gift from Dr. Jean-Christophe Bourdon (University of Dundee, Scotland, UK).

For the generation of the stable LHCN-M2 cell line, knocked-out of FLp53 or total p53, small guide RNAs (sgRNA) were designed in order to selectively target the ATG codon in position 1 (to knock-out only FLp53) or in position 40 (to knock-out total p53). BsmBI linkers were added to sgRNAs and the oligonucleotides were then

annealed by incubation for 3 min at 90°C and 15 min at 37°C and ligated in plentiCRISPR v2 vector (2). Insertion of sgRNA was confirmed by sequencing. The use of plentiCRISPR v2, which is constructed around a 3rd generation lentiviral backbone, allows the simultaneous infection/transfection of the vector for the expression of Cas9 and gRNA and for the selection of puromycin resistance. For the generation of the A549 stable cell line and knocked-out of endogenous FLp53, sgRNA were designed using the GPP (Genetic Perturbation Platform, Broad Institute) sgRNA Designer tool (CRISPRa/i), available on the https://portals.broadinstitute.org/gpp/public/analysis-tools/sgrna-design-crisprai site. sgRNAs, designed close to the first p53 promoter, were annealed as described above and inserted into the pLV hU6-sgRNA hUbC-dCas9-KRAB-T2a-Puro vector (3), allowing the expression of defective the Cas9 enzyme (dCas9) fused to the Krüppel-associated box (KRAB) transcriptional repressor (dCas9-KRAB). plentiCRISPR v2 was a gift from Feng Zhang (Addgene, Watertown, MA, USA, plasmid #52961; http://n2t.net/addgene:52961; RRID:Addgene_52961), and pLV hU6-sgRNA hUbC-dCas9-KRAB-T2a-Puro was a gift from Charles Gersbach (Addgene, plasmid #71236; http://n2t.net/addgene:71236; RRID:Addgene_71236). Small guide cloning sequences are listed in *SI Appendix*, Fig. S7.

**Quantitative RT-PCR**

Total RNAs were extracted using the NucleoSpin® RNA Plus Kit (Macherey Nagel, Düren, Germany) according to the manufacturer's protocol. RT-PCR reactions were performed with the PrimeScript RT Reagent Kit (Takara Bio Europe, Saint-Germain-en-Laye, France). 500 ng total RNA was reverse-transcribed using the following program: 37°C for 15 min and 85°C for 5 sec. For expression studies, the

target transcripts were amplified on the LightCycler®2.0 apparatus (Roche Applied Science, Indianapolis, IN, USA), using the Premix Ex Taq probe qPCR Kit (Takara Bio Europe), according to the manufacturer's instructions. Expression of target genes was normalized against TATA binding protein (TBP) and beta-glucuronidase (GUSB) genes, used as housekeeping genes. The amount of target transcripts, normalized against the housekeeping gene, was calculated using the comparative $C_T$ method. A validation experiment was performed, in order to demonstrate that the efficacy of target and housekeeping genes was almost equivalent. Primer sequences are available in *SI Appendix*, Fig. S7.

**Western blot analysis**

For immunoblotting analysis, cells were lysed by sonication in SDS buffer (10 mM Tris-HCl pH 7.4, 10% glycerol, 5% SDS, 1% TX-100, 100 mM DTT) in the presence of protease inhibitor cocktail (Roche Applied Science). Protein extracts (20-50 µg per lane) were loaded onto 4-15% SDS-polyacrylamide gels (Biorad, Hercules, CA, USA) and blotted onto nitrocellulose sheets using the Trans-Blot Turbo Transfer System (Biorad). Filters were blocked with 10% non-fat dried milk in PBS/0.1% Tween 20 (PBS-T) for 2 hours and incubated overnight at 4°C with the following antibody: rabbit monoclonal antibody α-netrin-1 (1:1000 dilution, #ab126729, Abcam, Cambridge, UK,); rabbit polyclonal antibody α-p21 (1:2000, clone C-19, #sc-397, Santa Cruz Biotechnology, Dallas, TX, USA,); mouse monoclonal antibody α-p53 (1:1000, clone DO-1, #sc-126, Santa Cruz Biotechnology); mouse monoclonal antibody α-p53 (1:500, clone Pab 1801, #sc-98, Santa Cruz Biotechnology); mouse monoclonal antibody α-GAPDH (1:1000, clone 0411, #sc-47724, Santa Cruz Biotechnology); rabbit polyclonal antibody α-HA (1:5000, #H6908, Sigma-Aldrich); rabbit monoclonal

antibody α-BAX (1:1000, clone D2E11, #5023, Cell Signaling, Danvers, MA, USA); rabbit monoclonal antibody α-Ku80 (1:1000, clone C48E7, #2180, Cell Signaling); mouse monoclonal antibody α-β-actin, HRP-conjugated (1:10000, clone BA3R, #MA5-15739-HRP, Life Technologies); mouse monoclonal antibody α-p53 (1:1000, clone DO-11, #MCA1704, Biorad); rabbit monoclonal antibody α-UNC5B (1:1000, clone D9M7Z, # 13851, Cell Signaling). After three washes with PBS-T, filters were incubated with the appropriate HRP-conjugated secondary antibody (1:10000, Jackson ImmunoResearch, Suffolk, UK) for 1 h. Detection was performed using the West Dura Chemiluminescence System (Life Technologies). Membranes were imaged on the ChemiDoc Touch Imaging System (Biorad).

**Reporter assay**

Stable A549 cells inducible for FLp53 or ∆40p53 were plated in 12-well plates and transfected with the different firefly luciferase reporters containing wild-type or p53-mutated netrin-1 promoter constructs. 24 h after transfection, cells were treated with 2 µg/mL doxycycline and further incubated for 24 h. All transfections were performed in triplicate and the Dual-Luciferase Reporter Assay system (Promega, Charbonnieres, France) was carried out 48 h after transfection according to the manufacturer's protocol, using the Infinite F500 apparatus (Tecan, Männedorf, Switzerland). As an internal control of transfection efficacy, the Renilla luciferase encoding plasmid (pRL-CMV, Promega) was co-transfected and for each sample firefly luciferase activity was normalized against the Renilla luciferase activity.

**Chromatin immunoprecipitation assay**

Stable H1299 cells inducible for Δ40p53 were treated with doxycycline for 24 h and collected by enzymatic detachment. Cells were then cross-linked with 1% formaldehyde/methanol solution (Sigma-Aldrich) in PBS. After 30 min incubation at 4°C, the cross-link reaction was blocked by centrifugation and three washes with PBS. After lysis with buffer L1 (50 mM Tris-HCl pH 8.0, 2 mM EDTA, 0.1% NP40, Glycerol 10%) supplemented with protease inhibitor cocktail (Roche Applied Science), nuclei were centrifugated and resuspended in buffer L2 (50 mM Tris-HCl pH 8.0, EDTA 5mM, 1% SDS). Next, chromatin was shared by sonication (Branson 450 Digital Sonifier, 3 mm microtip, Branson Ultrasonics, Danbury, CT, USA) and diluted 10 times with buffer DB (50 mM Tris-HCl pH 8.0, 5 mM EDTA, 200 mM NaCl, 0.5% NP40). After preclear extract for 2 h with salmon sperm-saturated protein G (ssPrG, Cell Signaling), Δ40p53-HA complexes were immunoprecipitated over-night using 2 µg of HA antibody (BioLegend). Immunocomplexes were collected with ssPrG, and following four washes with buffer WB (20 mM Tris-HCl pH 8.0, 2 mM EDTA, 0.1% SDS, 1% NP40, 500 mM NaCl) and three washes with TE buffer (10 mM Tris-HCl pH 8.0, 1 mM EDTA), antigen/antibody complexes were extracted with buffer EB (10 mM Tri-HCl pH 8.0, 1 mM EDTA, 2% SDS). Protein-DNA cross-links were reverted by adding 6 µl of 5M NaCl and 2 µl of proteinase K at 20 mg/mL and by incubation 2 h at 65°C. DNA was then purified using NucleoSpin® Gel and a PCR Clean-up kit (Macherey Nagel), according to the manufacturer's protocol. Quantitative real-time PCR analysis of regulatory and control sequences in input samples and immunoprecipitated DNA was performed using the ONEGreen FAST QPCR PREMIX (Ozyme, Saint Cyr L'Ecole, France) in the CFX96 apparatus (Biorad). Sequences of primers used for ChIP analysis are illustrated in *SI Appendix*, Fig. S7.

**Cell Death Assays**

For DNA fragmentation analysis (SubG1), LHCN-M2 cell lines were plated onto 6-well plates at a density of $1.5*10^5$ cells per well. The following day, cells were transfected with siRNA, as described above, and incubated in serum-free medium for 48 h. For SubG1 analysis of A549 cell lines, cells were plated onto 6-well plates at a density of $5.0*10^5$ cells per well and transfected with siRNA the day after. 24 h later, transfected cells were plated again in complete medium onto 6-well plates at a density of $1.5*10^5$ cells per well. The following day, cells were treated with doxycycline in serum-free medium and further incubated for 48 h. Cells were then collected, fixed in 70% ethanol and incubated at -20°C for at least one night. Subsequently, cells were washed twice with PBS and incubated for 5 min at 37°C in PBS containing 0.1% TX-100 and 2 µg/mL 4′,6-diamidino-2-phenylindole (DAPI). DNA content was evaluated using the NucleoCounter NC-3000 system (ChemoMetec A/S, Allerød, Denmark).

For AnnexinV and propidium iodide (PI) double staining, LHCN-M2 cell lines were seeded onto 6-well-plates at a density of $2.5*10^5$ cells per well. The following day, cells were transfected with siRNA and incubated in serum-free media for 72 h. Cells were then harvested, washed with PBS and incubated for 15 minutes in Annexin V buffer containing allophycocyanin (APC) conjugated to Annexin V and PI (BioLegend, San Diego, CA, USA). Annexin V positive cells were then evaluated by fluorescence activated cell sorting (FACS) on FACSCanto II (BD Biosciences, San Jose, CA, USA).

Caspase-3 activity assay was performed as described previously (1) and was calculated from a 1 h kinetic cycle reading on a spectrofluorometer (405 nm / 510 nm, Infinite F500, Tecan).

**Xenografts *in ovo***

Fertilized white Leghorn chicken eggs were incubated at 38°C with 60% humidity. A small window was made in the shell on day 3 of chick embryo development under aseptic conditions, in order to aspire liquid inside. Windows were then sealed and eggs incubated for further seven days. For stable A549 cells, inducible for ∆40p53, ten million of cells were suspended in 50 µL complete medium and 50 µL of Matrigel Matrix (Corning, Massachusetts, USA) and seeded on 10 days-old chick chorioallantoic membrane (CAM). Netrin-1 neutralizing antibody NP137 and relative control NP001 (10 µg/mL) (Netris Pharma, Lyon, France) and doxycycline (2 µg/mL) were mixed together with cells and Matrigel before seeding. Eggs were then resealed and incubated for further seven days. For HCT116 cells wild-type or knock-out for FLp53, ten million of cells were engrafted as described above and treated with NP137 and NP001 antibodies (10 µg/mL) for seven days. Then, tumors where resected and weighted, and the tumor areas were measured with AxioVision Release 4.6 software (Carl Zeiss France, Marly le Roi, France). All ex ovo experiments were performed in accordance with relevant guidelines and regulations of animal ethics committee (Authorization APAFIS n°: 28723; accreditation of laboratory animal care by CECCAP, ENS Lyon-PBES, France).

**Xenografts in *nude* mice**

5-week-old female athymic *nude* Foxn1$^{nu/nu}$ mice were obtained from Janvier Labs (Saint Bertevin, France). The mice were maintained in a Specific and Opportunistic Pathogen-Free (SOPF) animal facility. Parental (n = 10) or stable (n = 20) A549 cells inducible for ∆40p53 were implanted by subcutaneous injection of 5*10$^6$ cells suspended in 100µl of PBS into the right flank of *nude* mice. When tumors

reached approximatively a volume of 70 $mm^3$, mice were randomly separated in three groups (n = 10 for each group). Mice engrafted with parental A549 cells were intravenously injected three times per week with 100 µl of PBS for 36 days. Mice bearing tumors from stable A549 cells inducible for Δ40p53 were treated with 1 mg/ml of doxycycline (Sigma-Aldrich) in drinking water and intravenously injected three times per week with 10 mg/Kg of anti-netrin-1 or isotypic control antibodies for 36 days. Tumor size was measured three times per week with a caliper. Tumor volume was calculated according to the formula v= 0.5 x (l x w2), where v is volume, l is length, and w is width. All experiments were performed in accordance with relevant guidelines and regulations of animal ethics committee (Authorization APAFIS n°: 28723; accreditation of laboratory animal care by CECCAP, ENS Lyon-PBES, France).

**Immunohistochemical staining**

For histological examination of tumors engrafted in *nude* mice, endpoint tumors were fixed in 10% buffered formalin and embedded in paraffin. 4-µm-thick tissue sections of formalin-fixed, paraffin-embedded tissue were prepared according to conventional procedures. Sections were then stained with hematoxylin and eosin and examined with a light microscope. Immunohistochemistry was performed on an automated immunostainer (Ventana Discovery XT, Roche, Meylan, France) using Omnimap DAB Kit according to the manufacturer's instructions. Sections were incubated with a rabbit anti-cleaved caspase-3 antibody (diluted at 1:500, #9661S, Cell Signaling). HRP-conjugated anti-rabbit antibody was applied on sections. Staining was visualized with DAB solution with 3,3′-diaminobenzidine as a chromogenic substrate. Then, the sections were counterstained with Gill's hematoxylin. Finally, sections were scanned with panoramic scan II (3D Histech, Budapest, Hungary) at 20X.

Quantification of caspase-3 positive cells was performed with HALO software and adapted algorithms cytonuclear v2.0.8 6 (Indica Labs, Albuquerque, NM, USA). All immunohistochemical staining and analysis were performed by the Research Pathology Platform East (Plateforme Anatomopathologie Recherche, Université de Lyon, Université Claude Bernard Lyon 1, INSERM 1052, CNRS 5286, Centre Léon Bérard, Centre de recherche en cancérologie de Lyon (CRCL), Lyon, 69373, France).

**Patients and tumor samples**

For the melanoma cohort, 24 tumor samples were collected as previously described (4), from patients who had undergone surgery for skin melanocytic lesions between 2007 and 2011. The research protocol was approved by the Ethics committee of Saint Louis Hospital (Paris, France). 19 primary colorectal cancer tissue samples were obtained from the Biological Resource Centre (CRB, Centre de Resource Biologique) of Léon Bérard Centre (protocol number: BB-0033-00050) (Lyon, France). The research protocol was approved by CRB medical and scientific committee. All of the patients signed informed consent letters, as required by the French Bioethics law, approving the use of their samples for research.

**Statistical analysis**

The data reported are expressed as the mean ± S.D. of at least three independent determinations, each performed in triplicate. Statistical analysis was performed using the Two-way ANOVA or linear regression tests, using GraphPad Prism version 6.01 for Windows (GraphPad Software, La Jolla, CA, USA), except where indicated differently.

## References for SI citations


1. H. Wang *et al.*, The Proto-oncogene c-Kit Inhibits Tumor Growth by Behaving as a Dependence Receptor. *Molecular cell* **72**, 413-425 e415 (2018).
2. N. E. Sanjana, O. Shalem, F. Zhang, Improved vectors and genome-wide libraries for CRISPR screening. *Nature methods* **11**, 783-784 (2014).
3. P. I. Thakore *et al.*, Highly specific epigenome editing by CRISPR-Cas9 repressors for silencing of distal regulatory elements. *Nature methods* **12**, 1143-1149 (2015).
4. A. Boussouar *et al.*, Netrin-1 and Its Receptor DCC Are Causally Implicated in Melanoma Progression. *Cancer research* **80**, 747-756 (2020).

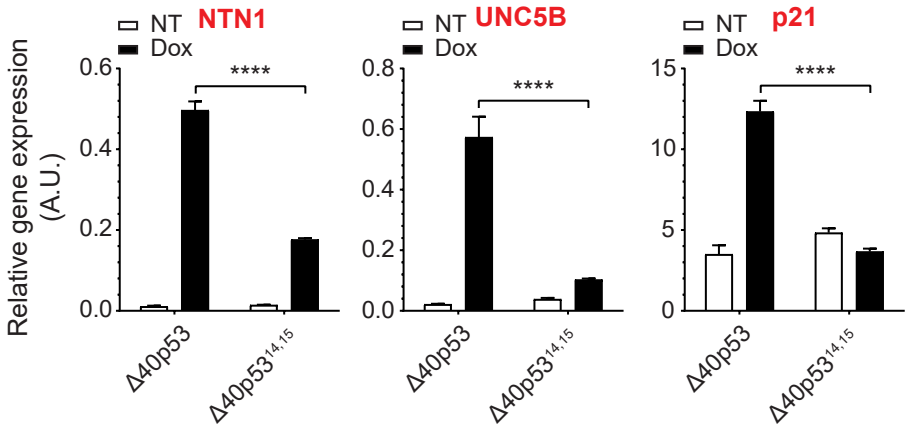


**Fig. S1.** Δ40p53-dependent netrin-1 induction requires Δ40p53 transcriptional activity. Stable A549 cell lines, inducible for wild-type or TAD-mutated Δ40p53 protein (Δ40p53$^{14,15}$), were treated with 2 µg/mL of doxycycline. Netrin-1, UNC5B and p21 gene expression was evaluated by quantitative RT-PCR. Data are represented as mean ± SEM (n = 3). $p < 0.001$; ****; Dox, doxycycline; NTN1, netrin-1; CTRL, control; A.U., arbitrary units.

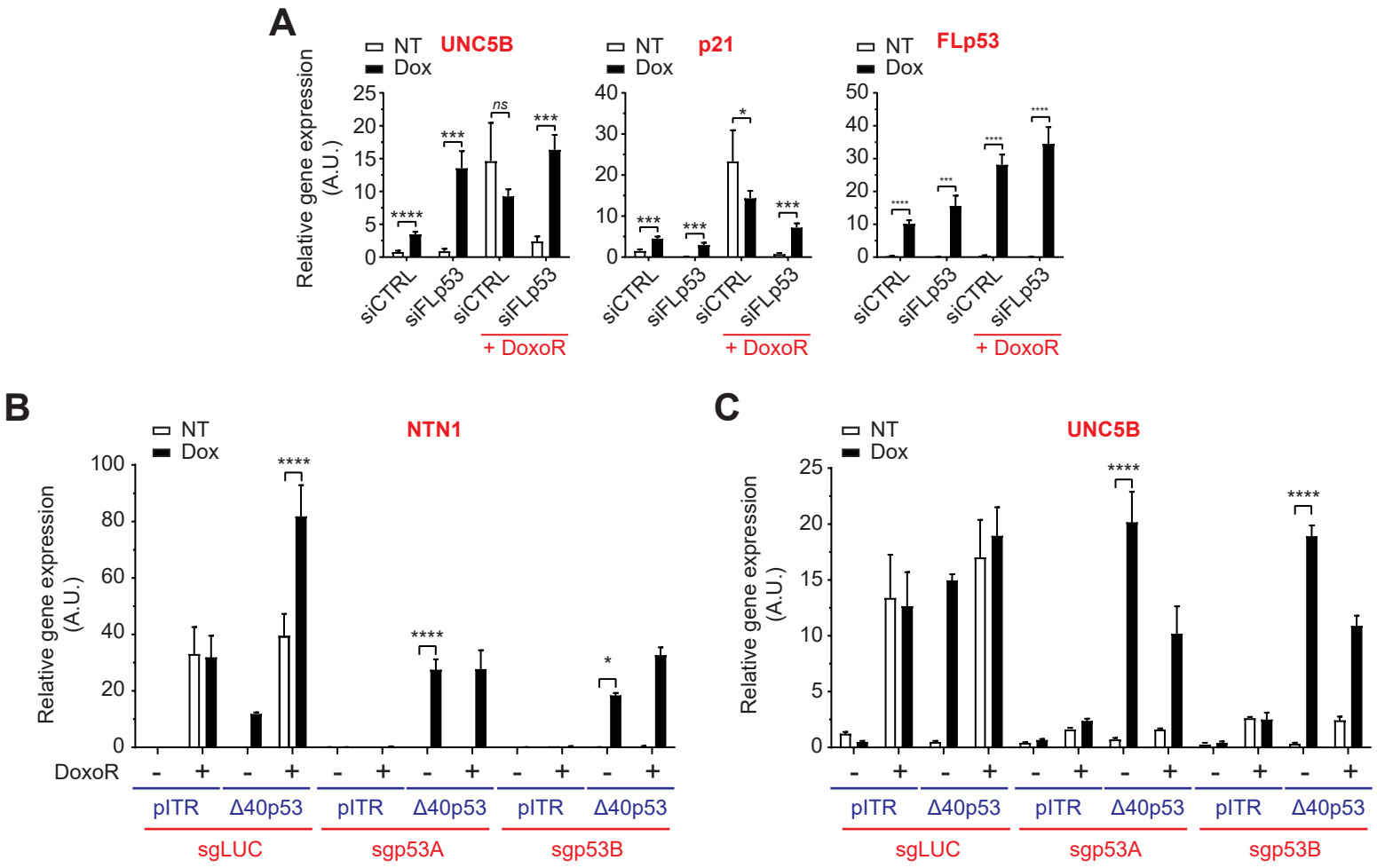


**Fig. S2.** Full-length p53 is not necessary for netrin-1 regulation by Δ40p53. (A) Silencing of endogenous p53 expression does not affect Δ40p53-dependent UNC5B up-regulation. Stable A549 cell lines, inducible for Δ40p53, were transfected with a scramble siRNA (siCTRL) or with a specific siRNA targeting exon 2 of the p53 gene (sip53). 24 h after transfection, cells were treated with doxorubicin or doxycycline for a further 24 h. UNC5B and p21 transcript levels were quantified by quantitative RT-PCR. p53 silencing efficacy was evaluated by quantitative RT-PCR, using full-length p53-specific primers (FLp53), designed in exon 2 of p53 gene. Gene expression was normalized using TATA-binding protein (TBP) and beta-glucuronidase (GUSB) genes, used as housekeeping genes. (B, C) Δ40p53-induced netrin-1 and UNC5B gene expression is not altered by knocking-down endogenous p53. A549 cells were infected using CRISPR/Cas9-modified pLV-hU6-sgRNA-hUbC-dCas9-KRAB-T2a-Puro plasmid, and stable cell lines were generated using firefly luciferase-control (sgLUC) or p53-specific (sgp53A and sgp53B) small guide RNAs. Endogenous p53 knocked out cell lines were then transfected with empty (pITR) or Δ40p53 sleeping-beauty plasmids. Stable A549 cell lines knocked out for p53 and inducible for Δ40p53 were treated with doxorubicin and doxycycline for 24 h. Netrin-1 (B) and UNC5B (C) transcript levels were assessed by quantitative RT-PCR. Data are presented as mean ± SEM (n = 3). ns, non-significant; *, $p < 0.05$; ***, $p < 0.001$; ****, $p < 0.0001$. CTRL, not treated, control cells; Dox, doxycycline; DoxoR, doxorubicin; NTN1, netrin-1; FLp53, full-length p53; sg, small guide.

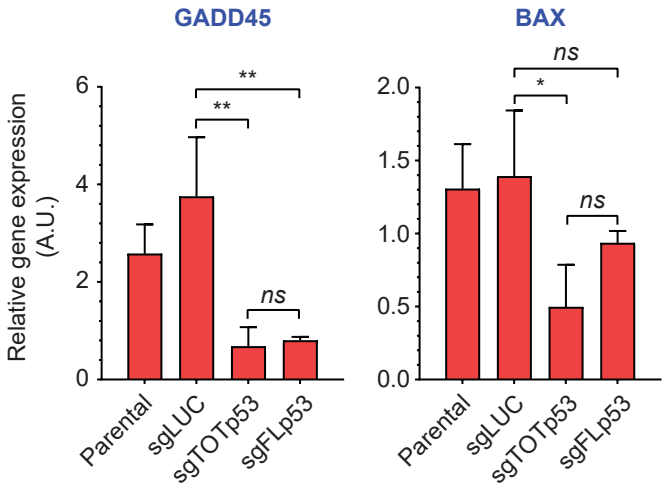


**Fig. S3**. Endogenous Δ40p53 affects GADD45 and BAX gene expression. Stable LHCN-M2 cells knocked out for p53 gene were generated using firefly luciferase-control (sgLUC), ATG1- (sgFLp53) or ATG40- (sgTOTp53) targeting sgRNAs. Expression levels of Growth Arrest and DNA Damage 45 (GADD45) and BAX transcripts were analyzed by quantitative RT-PCR. Results are presented as mean ± SEM (n = 3). ns, non-significant; *, $p < 0.05$.

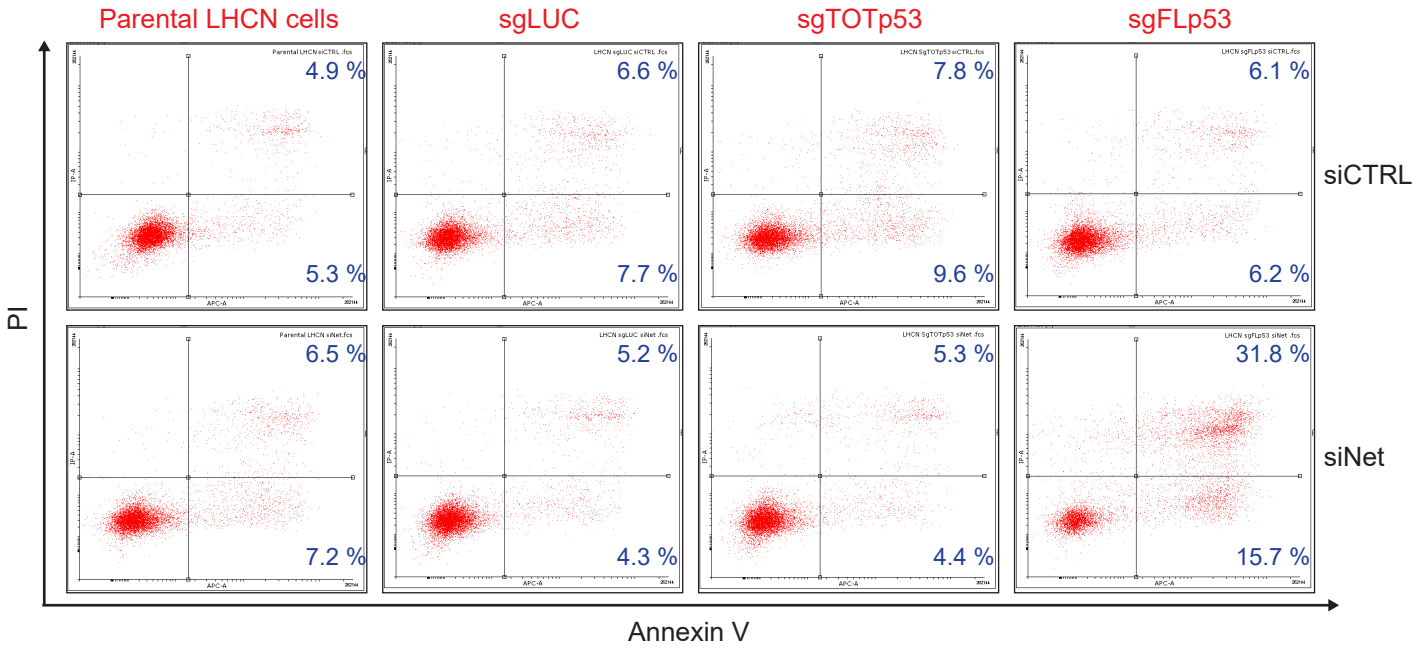


**Fig. S4.** Δ40p53 expression sensitizes cells to netrin-1 silencing-induced apoptosis. Parental or stable LHCN-M2 cells, infected with control (sgLUC), FLp53/Δ40p53 (sgTOTp53) or FLp53 only (sgFLp53) knock-out lentiviral constructs, were transfected with scramble (siCTRL) or netrin-1-specific (siNet) siRNAs. Induction of apoptosis was evaluated by Annexin V and PI double staining analyzed by flow cytometry. A representative experiment is shown. Number in blue denoted the percentage of Annexin V-positive cells for each condition. The bottom right quadrant indicated early apoptotic cells, whereas the upper right quadrant illustrated cells in late apoptosis.

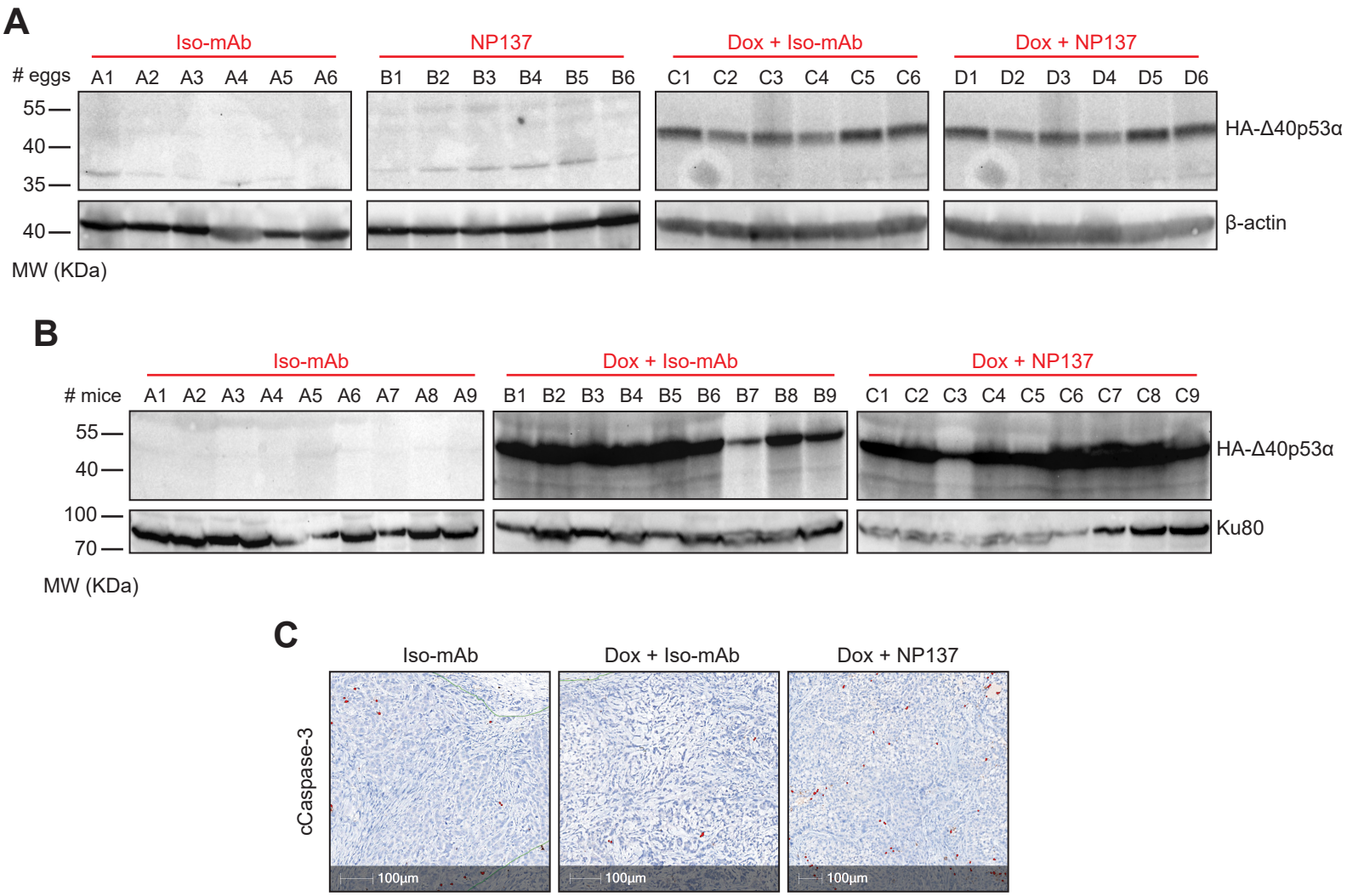


**Fig. S5.** Δ40p53 expression sensitizes cells to netrin-1 interference-induced tumor growth inhibition. (A) A549 cells were seeded in the CAM of E10 chick embryo, together with doxycycline (dox) and anti-netrin-1 (NP137) or control (Iso-mAb) antibodies. Seven days later, primary tumors were resected and lysed, and HA-tagged Δ40p53 expression was evaluated by Western blot, using anti-HA antibody. β-actin was used as housekeeping gene to normalize protein content. (B) Stable A549 cells inducible for HA-Δ40p53 were engrafted in nude mice. Once the tumor formed, mice were treated with anti-netrin-1 (NP137) or control (Iso-mAb) antibodies and watered with doxycycline (dox). 36 days after the start of treatment, mice were sacrificed and engrafted tumors resected and lysed. Induced Δ40p53 expression was then evaluated by Western blot, using anti-HA antibody. Ku80 antibody was used to normalize protein loading. (C) Anti-tumoral effect of NP137 antibody is associated with apoptosis induction. Engrafted tumors were resected 36 days after beginning treatments and apoptosis was evaluated by immunohistochemical staining of active caspase-3 (cCaspase-3). Representative images are displayed. MW, molecular weight; cCaspase-3, cleaved caspase-3.

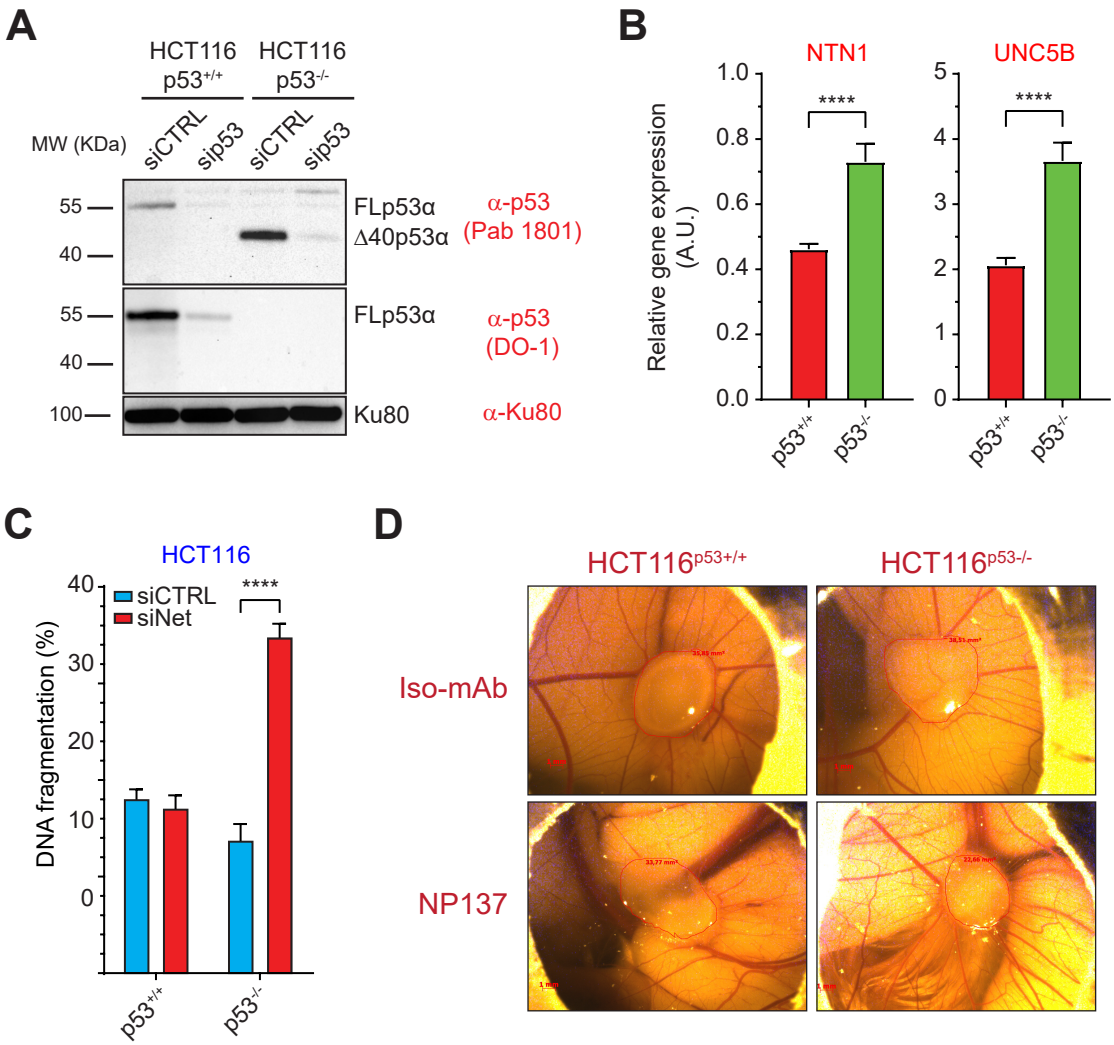


**Fig. S6.** Colorectal HCT116 cancer cell line deleted of FLp53 expresses endogenous Δ40p53α, and shows an increase of netrin-1 and UNC5B transcript levels, affecting sensitivity to netrin-1 inhibition. (A) HCT116 wild-type (HCT116-p53$^{+/+}$) or deleted for the second exon of p53 gene (HCT116-p53$^{-/-}$) were transfected with siRNA targeting the exon 7 of p53 gene (sip53). 48 h after transfection, protein levels of FLp53 and Δ40p53 were evaluated by western blot, using the Pab 1801 and DO-1 p53 antibodies. Ku80 antibody was used to normalize protein expression. (B) Netrin-1 and UNC5B transcript levels were evaluated in the two cell lines by quantitative RT-PCR (n = 11). Statistical analysis was obtained using the Mann – Whitney test. (C) Endogenous Δ40p53α expression in HCT116-p53$^{-/-}$ cells sensitizes to netrin-1 silencing. p53$^{+/+}$ and p53$^{-/-}$ HCT116 cells were transfected with siRNA targeting netrin-1. 48 h after transfection, apoptosis was evaluated by measuring DNA fragmentation rate (n = 3). (D) Wild-type or FLp53-knockout HCT116 cells were seeded in the CAM of E10 chick embryo, together with 10 µg/mL of anti-netrin-1 (NP137) or control (Iso-mAb) antibodies. Tumors were imaged after seven days and areas were measured. Representative images of primary tumors are shown (scale bar = 1 mm). Data in B and C are represented as mean ± SEM. ****, $p < 0.0001$. A.U., arbitrary units; mAb, monoclonal antibody; Iso, isotypic.

| qPCR primers | | | | |
|---|---|---|---|---|
| | *Forward primers* | | *Reverse primers* | |
| **Target** | **Name** | **Sequence** | **Name** | **Sequence** |
| **Netrin-1** | NTN1_for81 | gcaagcccttccactacg | NTN1_rev81 | gcatgcaggttgcagttaca |
| **UNC5B** | UNC5B_for28 | tgccaccgtcatcgtctac | UNC5B_rev28 | gttggagcagggtgacca |
| **FLp53** | TA_D40p53_for71 | ctttccacgacggtgaca | TA_D40p53_rev71 | tcctccatggcagtgacc |
| **p53** | p53TOT_for21 | tagtgtggtggtgccctatg | p53TOT_rev21 | cccatgcaggaactgttacac |
| **TBP** | TBP_for3 | cggctgtttaacttcgcttc | TBP_rev3 | cacacgccaagaaacagtga |
| **GUSB** | GUSB_for57 | cgccctgcctatctgtattc | GUSB_rev57 | tccccacagggagtgtgtag |
| **GADD45** | GADD45_for37 | gagagcagaagaccgaaagg | GADD45_rev37 | tgactcagggctttgctga |
| **BAX** | BAX_for57 | atgttttctgacggcaacttc | BAX_rev57 | atcagttccggcaccttg |
| **p21** | p21_for82 | cgaagtcagttccttgtggag | p21_rev82 | catgggttctgacggacat |

| ChIP primers | | | | |
|---|---|---|---|---|
| | *Forward primers* | | *Reverse primers* | |
| **Target** | **Name** | **Sequence** | **Name** | **Sequence** |
| **Netrin-1** | NetP-p53_F7 | cagaggtaaagtcccgaacgc | NetP-p53_R7 | agtttcgggcgcaggagag |
| **Netrin-1** | NetP-p53_F10 | cgggctgcgagacgaag | NetP-p53_R10 | ctcgcaccccaagtttcg |
| **Netrin-1** | NetP-K1_F3 | cctaagagctatgctgcctttc | NetP-K1_R3 | gttaaccatggtgacctgtgaaat |
| **p21** | p21-1354 For | cccacagcagaggagaaaga | p21-1354 Rev | catctcaggctgctcagagtc |

| small guide cloning primers | | | | |
|---|---|---|---|---|
| | *Forward primers* | | *Reverse primers* | |
| **Target** | **Name** | **Sequence** | **Name** | **Sequence** |
| **Luciferase** | sgLUC1_F | caccggggcatttcgcagcctaccg | sgLUC1_R | aaaccggtaggctgcgaaatgcccc |
| **p53** | sgRNAi_p53A_for | caccgtgggagcgtgctttccacga | sgRNAi_p53A_rev | aaactcgtggaaagcacgctcccac |
| **p53** | sgRNAi_p53B_for | caccgaagtctagagccaccgtcca | sgRNAi_p53B_rev | aaactggacggtggctctagacttc |

| siRNA | | |
|---|---|---|
| **Target** | **Name** | **Sequence** |
| **CTRL** | siCTRL-AP | aauucuccgaacgugucacgu |
| **FLp53** | siTAp53 | gcagucagauccuagcguc |
| **Netrin-1** | siNet-5' | aagcuggacgcagcaugaugc |

**Fig. S7.** Primer and siRNA sequences used for qPCR, ChIP analysis, small guide cloning and RNA interference